Pain-like behavior in the collagen antibody-induced arthritis model is regulated by lysophosphatidic acid and activation of satellite glia cells

Jie Su, Emerson Krock, Swapnali Barde, Ada Delaney, Johnny Ribeiro, Jungo Kato, Nilesh Agalave, Gustaf Wigerblad, Rosalia Matteo, Roger Sabbadini, et al.

Brain, Behavior, and Immunity 101 (2022) 214–230

Contents lists available at ScienceDirect

Brain Behavior and Immunity

journal homepage: www.elsevier.com/locate/ybrbi

Pain-like behavior in the collagen antibody-induced arthritis model is regulated by lysophosphatidic acid and activation of satellite glia cells

Jie Su [a,b,1], Emerson Krock [a,1], Swapnali Barde [c], Ada Delaney [a], Johnny Ribeiro [d], Jungo Kato [a], Nilesh Agalave [a], Gustaf Wigerblad [a], Rosalia Matteo [e], Roger Sabbadini [e,f], Anna Josephson [c], Jerold Chun [g], Kim Kultima [a,h], Olivier Peyruchaud [d], Tomas Hökfelt [c], Camilla I. Svensson [a,*]

[a] Department of Physiology and Pharmacology, Center for Molecular Medicine, Karolinska Institutet, 17177 Stockholm, Sweden
[b] Department of Medical Biochemistry and Biophysics, Division of Molecular Neurobiology, Karolinska Institutet, 17177 Stockholm, Sweden
[c] Department of Neuroscience, Karolinska Institutet, 17177 Stockholm, Sweden
[d] INSERM, U1033 Lyon, France
[e] LPath Inc, San Diego, United States
[f] Department of Biology, San Diego State University, 92182, United States
[g] Translational Neuroscience Initiative, Sanford Burnham Prebys Medical Discovery Institute, La Jolla, CA 92037, United States
[h] Department of Medical Sciences, Uppsala University, 75185 Uppsala, Sweden

ARTICLE INFO

Keywords:
Rheumatoid arthritis
Dorsal root ganglia
Lipid signaling
Autoantibodies
Inflammation
Neuropathic pain
Autotaxin
Enpp2

ABSTRACT

Inflammatory and neuropathic-like components underlie rheumatoid arthritis (RA)-associated pain, and lysophosphatidic acid (LPA) is linked to both joint inflammation in RA patients and to neuropathic pain. Thus, we investigated a role for LPA signalling using the collagen antibody-induced arthritis (CAIA) model. Pain-like behavior during the inflammatory phase and the late, neuropathic-like phase of CAIA was reversed by a neutralizing antibody generated against LPA and by an $LPA_{1/3}$ receptor inhibitor, but joint inflammation was not affected. Autotaxin, an LPA synthesizing enzyme was upregulated in dorsal root ganglia (DRG) neurons during both CAIA phases, but not in joints or spinal cord. Late-phase pronociceptive neurochemical changes in the DRG were blocked in *Lpar1* receptor deficient mice and reversed by LPA neutralization. *In vitro and in vivo* studies indicated that LPA regulates pain-like behavior via the LPA_1 receptor on satellite glia cells (SGCs), which is expressed by both human and mouse SGCs in the DRG. Furthermore, CAIA-induced SGC activity is reversed by phospholipid neutralization and blocked in *Lpar1* deficient mice. Our findings suggest that the regulation of CAIA-induced pain-like behavior by LPA signalling is a peripheral event, associated with the DRGs and involving increased pronociceptive activity of SGCs, which in turn act on sensory neurons.

1. Introduction

Rheumatoid arthritis (RA) is a chronic autoimmune disease that affects 0.5–1% of the global population and is characterized by pain and inflammation in multiple joints. Inflammation has been the primary target of RA treatment, with the assumption that once inflammation is controlled pain will reside. A number of disease-modifying antirheumatic drugs (DMARDs) are effective at controlling inflammation, but many patients continue to suffer from persistent pain (Altawil et al., 2016; Lee et al., 2011; Taylor et al., 2010). In fact, up to 65% of RA patients report dissatisfaction with pain management (Taylor et al., 2010). Joint pain is common in RA, but pain is also reported at remote, non-articular sites (Edwards et al., 2009; Pollard et al., 2012) and a number of recent studies have found evidence of neuropathic-like pain characteristics in up to 33% of RA patients (Ahmed et al., 2014; Koop et al., 2015; Sim et al., 2014). Taken together, these findings indicate RA-associated pain is not simply an outcome of inflammation (Altawil et al., 2016; Lee et al., 2011; Taylor et al., 2010) and that anatomical sites beyond joints are involved. A better understanding of the neuropathological mechanisms underlying RA-associated pain will help mitigate the unmet need to develop novel pain management strategies.

The collagen antibody-induced arthritis (CAIA) mouse RA model was

* Corresponding author at: Karolinska Universitetssjukhuset, Centrum för Molekylär Medicin, L8:03, Visionsgatan 18, 171 76 Stockholm, Sweden.
E-mail address: camilla.svensson@ki.se (C.I. Svensson).
[1] indicates that JS and EK are co-first authors.

https://doi.org/10.1016/j.bbi.2022.01.003
Received 15 August 2021; Received in revised form 14 December 2021; Accepted 7 January 2022
Available online 10 January 2022

developed based on the presence of anti-collagen type II autoantibodies in RA patients (Cook et al., 1996; Holmdahl et al., 1993; Kim et al., 2000; Lindh et al., 2014; Mullazehi et al., 2012) and the findings that rodents and non-human primates immunized with collagen type II develop an autoimmune response and joint pathology similar to human RA (Krock et al., 2018; Vierboom et al., 2005). CAIA is induced by injecting a cocktail of anti-collagen type II antibodies, which results in inflammation, and bone and cartilage erosion in the joints of the ankles and paws (Krock et al., 2018; Nandakumar and Holmdahl, 2007). We have previously reported that mice subjected to CAIA display pain-like behavior when the joints are inflamed and, remarkably, that the pain-like behavior persists despite resolution of the joint inflammation (Bas et al., 2012). Diclofenac, an NSAID, and gabapentin, a drug that is used to treat neuropathic pain, both attenuate pain-like behavior during the inflammatory phase, but only gabapentin has an effect during the late phase (Bas et al., 2012). Furthermore, CAIA also leads to long-lasting, pain-related changes in DRGs, such increased expression of α2δ1, P2X3, galanin and the nerve injury markers ATF3 and GAP43. Long term changes in protein expression of these and other factors in the dorsal root ganglia (DRG) have been coupled to maintenance of hypersensitivity in a number of experimental models of neuropathic pain (Bas et al., 2012; Su et al., 2015). Thus, there are indications of multiple overlapping mechanisms, including a neuropathic pain-like component in the CAIA model. As it replicates some of the complexities of RA-associated pain, this model has the potential to provide new insights into both the inflammatory and non-inflammatory mechanisms of RA-associated pain.

Lysophosphatidic acid (LPA) is a lipid mediator linked to neuropathic pain and inflammation. LPA is enzymatically generated from phospholipids, for example by the hydrolysis of lysophosphatidylcholine (LPC) to LPA by the extracellular enzyme autotaxin (ATX) (Choi et al., 2010; Umezu-Goto et al., 2002). LPA signals through at least six activating G protein-coupled receptors for LPA (LPA_{1-6}) (Choi et al., 2010; Kihara et al., 2014; Noguchi et al., 2009). In addition to being linked to pain, LPA signalling has physiological roles in cortical development, neurogenesis and myelination (Choi et al., 2010; Geraldo et al., 2021; Weiner et al., 2001; Weiner and Chun, 1999). In rodent models of nerve injury and osteoarthritis-induced pain, LPA is thought to drive the development of neuropathic-like pain through a number of processes: i) peripheral nerve demyelination (Inoue et al., 2004; McDougall et al., 2017; Ueda, 2017), ii) pain-related activation of astrocytes and (Ma et al., 2010a, 2010b), iii) increases of the neuropathic pain-linked voltage-dependent calcium channel α2δ1 subunit in the DRG (Inoue et al., 2004), and iv) central pain mechanisms (Lin et al., 2012). Interestingly, ATX and LPA_1 expression are elevated in synovial tissues from RA patients compared to controls (Miyabe et al., 2013; Nikitopoulou et al., 2012; Orosa et al., 2012). In fact, inhibiting LPA_1 signalling or ATX activity protects mice from joint destruction and inflammation during collagen-induced arthritis, *TNF*-transgenic arthritis and K/BxN serum transfer arthritis (Flammier et al., 2019; Miyabe et al., 2013; Nikitopoulou et al., 2013, 2012; Orosa et al., 2014). Thus, LPA signalling is linked to multiple forms of pain, particularly neuropathic pain, and RA joint pathogenesis and could be an integrator of RA autoimmunity and pain. However, the role of LPA signalling in RA-associated pain is poorly understood. Therefore, the aim of the current study was to investigate the potential role of LPA signalling in RA-associated pain using the CAIA model.

2. Methods

2.1. Animals, human DRG, CAIA induction and drug treatment

2.1.1. Animals:

Wild type male CBA mice were obtained from SCANBUR AB (Stockholm, Sweden) or Janvier (France). Mice were housed 4–6 per cage under standard conditions with a 12/12 h-light/dark cycle and food and water were available ab libitum. The experiments complied with the Swedish policies for the use of research animals and were approved by the local ethical committees; Stockholm's Norra djurförsöksetiska nämnd, permit no. N253/13 in Sweden, and the Institutional Animal Care and Use Committee of the Université Claude Bernard Lyon in France. *Lpar1*$^{-/-}$ mice were from the Peyruchaud group at INSERM, Lyon, France, originally developed on a C57Bl/6 background and backcrossed >12 times with BALB/c female mice (Contos et al., 2000; David et al., 2014). Due to small litter sizes, psychiatric illness-like behaviors and low survival rates (Contos et al., 2000; Harrison et al., 2003) we only used Lpar1$^{-/-}$ for immunohistochemical experiments in which Lpar1$^{-/-}$ and littermate WT could be paired for saline, CAIA + control Ab and CAIA + 504B3 experiments.

2.1.2. Human DRGs

A human dorsal root ganglion was obtained from a 48-year old female subject who consented to and donated her organs for transplantation surgery following approval of the local Ethical Committee and written consent from next of kin.

2.1.3. CAIA induction

CAIA was induced with i.v. injection of 1.5 mg anti-CII arthritogenic monoclonal antibody (Ab) cocktail (Chondrex Inc, Redmond, WA) on day 0 followed by 30 μg LPS (Chondrex Inc) intraperitoneally (i.p.) on day 5 (Nandakumar and Holmdahl, 2007). Control mice received 150 μl saline i.v. on day 0 and 100 μl saline i.p on day 5.

2.1.4. 504B3 pretreatment

CAIA mice received either a neutralizing monoclonal IgG2b antibody generated against LPA (504B3) (CAIA + 504B3, 2 or 10 mg/kg, Lpath Inc, San Diego, CA) or an isotype matched mouse monoclonal control antibody (CAIA + CTL Ab, 10 mg/kg, IgG2b, LPath Inc.) subcutaneously (s.c.) twice weekly, starting 8 days prior to CAIA induction (Day 0) and continuing until day 15 (total 8 injections). 504B3 is also commercially available from Echelon Biosciences. Vehicle control animals received 100 μl sterile saline s.c. (CTL + saline). Of note, the selectivity and affinity of 504B3 in blood and DRG have not been addressed in this study. Based on ELISA (Goldshmit et al., 2012) and a kinetic exclusion assay (Crack et al., 2014) 504B3 is selective for LPA but a free solution binding assay measured in a compensated interferometric reader found that 504B3 binds 18:1 LPC and 18:1 PA in addition to 18:1 LPA (Ray et al., 2021).

2.1.5. 504B3 post-treatment

Starting 12 days after CAIA induction (Day 0), mice were injected twice a week with 504B3 or control Ab (10 mg/kg and 2 mg/kg) s.c. through day 43 (11 injections total). Following the last injection, no injections were done for a 14-day washout period. After the drug washout, the mice were placed into new treatment groups, whith the first injection taking place day 57 after CAIA induction, and then injected twice a week until day 70 for a total of 7 injections. The former CAIA + saline group received 10 mg/kg 504B3, the CAIA + 504B3 group received the control antibody, the CAIA + CTL Ab group received saline, and the CTL + saline group continued to receive saline.

2.1.6. Ki-16425 post-treatment

The $LPA_{1/3}$ inhibitor Ki-16425 was dissolved in PBS with 10% DMSO. 20 mg/kg or vehicle were delivered subcutaneously daily, beginning 14 days after CAIA induction until the end of the experiment.

2.1.7. Intraarticular LPA injection

For i.a. injections mice were anesthetized with isoflurane (induction, 5%; maintenance, 2.5%), LPA (Avanti Polar Lipids, 250 pmol in 5 μl PBS containing 0.1% fatty acid free BSA(Sigma-Aldrich)) or 0.1% fatty acid free BSA in PBS or PBS (three groups: LPA, BSA and PBS) were injected into the ankle joint using a 29-G needle connected via tubing to a

Hamilton syringe.

2.2. Analyses of pain-like behavior

Testing of pain-like behavior was carried out in a dedicated behavior testing room on the indicated days. For mechanical, cold and heat hypersensitivity measurements the mice were habituated to the test environment twice prior to baseline assessment. Baseline measurements were taken three times on separate days and animals were then randomly assigned to control or CAIA groups and to antibody treatment groups. Experimenters were blind to arthritis status and treatment group.

2.2.1. Mechanical sensitivity

Mechanical hypersensitivity was assessed by the paw withdrawal response to von Frey optiHair filaments (Marstock OptiHair, Schriesheim, Germany) using the up–down method to calculate the 50% probability withdrawal threshold as previously describe (Chaplan et al., 1994). A series of filaments with a logarithmically incremental increasing stiffness of 0.5, 1, 2, 4, 8, 16 and 32 mN (subsequently converted to grams) were applied to the plantar surface of the hind paw and held for 2–3 s. A 4 g filament cut-off was used to avoid tissue damage and brisk paw withdrawal was considered a positive response.

2.2.2. Heat sensitivity

A Hargreaves-type testing device (UARDG, Department of Anesthesiology, University of California, San Diego) was used to assess heat hypersensitivity as previously described (Dirig et al., 1997; Svensson et al., 2005). Briefly, mice were placed in plexiglass cubicles on a glass surface maintained at 25 °C. The thermal nociceptive stimulus originates from a projection bulb (50 W bulb) below the glass surface and the stimulus is delivered separately to one hind paw at a time. A timer is activated by the light source, and automatically turned off by a motion sensor. Latency was defined as the time required for the paw to show a brisk withdrawal. Each hind paw was tested three times and the average withdrawal latency calculated.

2.2.3. Cold sensitivity

Cold sensitivity was measured by assessing the response to acetone. A single drop of acetone was applied to the plantar surface of the hind paw by forming a bubble of acetone with a syringe. The behavioral response of the mouse to acetone was then monitored for 60 s. In a single testing session, each paw was tested three separate times. Responses were graded on a four-point scale defined (Flatters and Bennett, 2004). Based on the time spent expressing nocifensive behavior the following scores were determined: 0 for no response, 1 if the total reaction time did not exceed 1 s, 2 if the reaction time was between 1 and 3 s, 3 if the total reaction time was between 3 and 10 s, and 4 if the total reaction time exceed 10 s (Su et al., 2014). The average score of the two hind paws was used.

2.3. qPCR

2.3.1. RNA isolation and reverse transcription

Animals were deeply anesthetized (5% isoflurane, Baxter Medical AB, Stockholm, Sweden) on day 15 and 45 after arthritis induction, decapitated, and the spinal cord, L4-L5 DRGs and ankle joints were collected. The tissues were immediately flash frozen and stored at −70 °C until analysis. For gene expression analysis of cell cultures, cells were lysed using TRIzol reagent (Invitrogen, Carlsbad, CA) for immediate use. Tissues were placed in TRIzol and RNA was extracted from tissues and cell cultures according to the manufacturer's instructions. RNA was reverse transcribed into cDNA using Multiscribe™ Reverse Transcriptase (Applied Biosystems). Quantitative real-time PCR analysis was performed using a StepOnePlus instrument (Applied Biosystems) with TaqMan™ Fast Advanced Master Mix (Applied Biosystems) and validated TaqMan Gene Expression Assays (Table 1, Applied Biosystems). As indicated in the figure legends, data were either analyzed with the standard curve method and presented as the percentage of controls (Boyle et al., 2003), analyzed with the $2^{-\Delta Ct}$ method and presented as relative expression, or analyzed with the $2^{-\Delta\Delta Ct}$ method and presented as fold difference compared to controls (Livak and Schmittgen, 2001). In all cases genes of interest were normalized to *Hprt1*.

2.4. Cell culture

DRG cultures were established using a modified protocol from Malin *et. al* (Malin et al., 2007). Adult male CBA mice were deeply anesthetized with isoflurane and euthanized by decapitation. Approximately 30 DRGs were removed per mouse and then digested in a 37 °C incubator, with 3 mL papain (Worthington, USA) for 30 min and then with 1.5 mL Collagenase type II (Worthington) and 1.5 mL Dispase II (Sigma). After digestion, ganglia were transferred to a 15 mL conical centrifuge tube with either L15 medium containing 10% fetal bovine serum (FBS, Fisher Scientific, Pittsburgh, PA) and 100 units/ml penicillin–streptomycin (Sigma) for DRG neuronal cultures or F12 medium supplemented with 100 units/ml penicillin–streptomycin and 10% FBS for SGC cultures. Ganglia were triturated until the suspension was homogeneous and the single cell suspensions were then filtered through a cell-strainer (100 μm, BD Biosciences, Bedford, MA). For DRG neuronal cultures the cell suspension was incubated for 90 min in 6 cm dishes to allow some glia cells to attach and the supernatant was removed and 200 μl/well of supernatant containing neurons was added to 48-well plates precoated with L-type poly-l-lysine and laminin (Sigma). For SGC cultures, single cell suspensions were placed in uncoated, 24-well plates (Sarstedt, Germany) and after 90 min the supernatant was removed, leaving only cells that adhered to the plastic, primarily glia. Cells were cultured in an incubator at 37 °C and 5% CO_2. Media was changed every 2–3 days.

2.5. Western blot

Primary DRG neuron culture samples were collected in 50 μl iced lysis buffer (0.5% Triton X-100, 50 mM Tris, 150 mM NaCl, 1 mM EDTA and 1% SDS, pH 7.4) containing 1% protease inhibitor and phosphatase inhibitor cocktail 1 and 2 (Sigma). The total protein concentration was determined with a BCA Protein Assay Kit (Pierce, Rockford, IL) and 2 μg of denatured protein was separated by electrophoresis on a NuPAGE 3–8% Tris-Acetate gel and then transferred by iBlot2 Dry Blot system (Life Technologies). Membranes were then blocked for 1 h in 5% non-fat milk in TBS.T (0.1% Tween 20) at room temperature and then incubated over night with primary antibodies against α2δ1 (1:500, Sigma) overnight at 4 °C.

After washing, membranes were probed with secondary antibodies conjugated to horseradish peroxidase, which were then detected with SuperSignal West Femto reagents (Thermo, Rockford, IL) and imaged with a ChemiDoc™ MP system (Bio-Rad Laboratories, Inc., Hercules, CA). Membranes were stripped with Re-Blot Solution (Millipore) and reprobed with anti-GAPDH antibody (1:5000, Abcam). Band intensity of α2δ1 was quantified using Image Lab™ 5.2.1 software (Bio-Rad), normalized to GAPDH and then compared to levels detected in the vehicle treated samples.

2.6. Immunohistochemistry

2.6.1. DRGs

Mice were deeply anesthetized with sodium pentobarbital (60 mg/kg) and perfused transcardially with 20 mL of pre-warmed (37 °C) saline, followed by 20 mL of pre-warmed and then 50 mL of cold 4% paraformaldehyde containing 0.2% picric acid in 0.16 M phosphate buffer (pH 7.2–7.4). L4/L5 DRGs were dissected and post-fixed in the same fixative for 90 min at 4 °C. After cryoprotection in 10% sucrose in 0.1 M PBS containing 0.01% sodium azide (VWR International) and

0.02% bacitracin (Sigma, St. Louis, MO) for 48 h, the tissue was embedded with OCT (HistoLab, Gothenburg, Sweden), frozen with liquid carbon dioxide and sectioned on a CryoStar NX70 cryostat (Thermo Scientific, Walldorf, Germany) at 12 μm thickness.

All antibody details are found in **supplemental table 2**. Prior to incubation with blocking or antibody solutions mounted sections were dried at RT for at least 30 min. Sections that were probed only for α2δ1 or LPA_1 were incubated with the respective antibodies diluted in phosphate-buffered saline (PBS) containing 0.2% (wt/vol) BSA (Sigma) and 0.3% Triton X-100 (Sigma) in a humidity chamber at 4 °C for 48 h. Immunoreactivities were visualized using the TSA Plus kit (PerkinElmer, Waltham, MA) as previously described. Sections probed for ATX were incubated with an antibody against ATX for 40 h, visualized with a secondary antibody and co-labelled with Neurotrace 435/455 (Thermofisher). For double-labelling, sections of mouse or human ganglia already probed for LPA1 using TSA were rinsed with PBS and then incubated with antibodies against α2δ1 for 48 h, or antibodies against GS or Iba1 for 24 h, in a humidity chamber at 4 °C. Slides were then probed with appropriate secondary antibodies. Single labeled sections were counterstained with 0.001% propidium iodide (PI, Sigma) for 10 min at RT. Double-labelled sections were counterstained with DAPI (Sigma) for 15 at RT. After rinse in PBS, the sections were mounted with DABCO medium of ProLong™ Gold Antifade Mountant with DAPI (Thermoscientific).

2.6.2. Neuronal cell culture:

12 mm coverslips (Fisher Scientific) were coated with poly-l-lysine and laminin (Sigma) in 24-well plates prior to seeding neurons. Following the end of LPA treatment, DRG cultures were washed with cold PBS and then fixed in cold fixative (4% PFA containing 0.2% picric acid in 0.16 M phosphate buffer, pH 7.4) for 15 min. The cells were then washed 3 times with PBS, 15 min for each. For staining, the fixed cells were permeabilized with 0.3% Triton X-100/PBS for 15 min, blocked with 5% normal goat serum in 0.3% Triton X-100/PBS for 30 min at RT and then incubated with α2δ1 antibody and mouse anti-MAP2 monoclonal antibody. Following washing, coverslips were then incubated with the appropriate secondary antibodies at room temperature. The α2δ1 positive neurons were counted, and the percentage of α2δ1+/MAP2 + cells was calculated.

2.6.3. Imaging and Quantification:

Representative images were captured from a one airy unit pinhole setting using a LSM710 or LSM800 laser-scanning confocal microscope (Carl Zeiss, Jena, Germany) with ZEN2012 software (Zeiss). Emission spectra for each dye were limited as follows: DAPI (<480 nm), Fluorescein (505–540 nm), Cy3 (560–610 nm), PI (590–680 nm). In selected cases (as indicated in the figure legend), projection images were merged from orthogonal scanning (*z*-stack) using step-intervals of 1.0 μm. Images were processed using ZEN2012 software.

For quantification of α2δ1, ATX, LPA1, GFAP, P2X3 and Galanin whole DRGs were tile scanned from 3 to 5 randomly selected sections with a minimum of 50 μm in between sections. Pixel intensity and the % area that was immunoreactive were quantified using ImageJ.

2.7. In situ hybridization

2.7.1. Probe synthesis:

Mouse and human *Lpar1* RNA probes were synthesized using sequence specific primers (mouse *Lpar1*: forward primer 5′-ATGAGGACACTCCTGTACTTAACA-3′; reverse primer 5′-GAAAGGCATACTGAATACACACAC-3′, human *Lpar1*: forward primer 5′-CCCCAGTTCACAGCCATGAATGAACC-3′; reverse primer 5′-CATGCGGAAAACCGTAATGTGCCTCT-3′) and cDNA obtained from mouse brain and human hypothalamus, respectively. The purified PCR products were subcloned into PCR1II-TOPO vector (Invitrogen) and the orientation was confirmed by nucleotide sequencing (KIGene, Stockholm, Sweden). The plasmids were then linearized and reverse transcribed by T7/Sp6 RNA polymerase (Life Technologies, Carlsbad, CA) in the presence of ^{35}S-UTP (PerkinElmer, Boston, MA). The generated probes were purified using NucAway spin columns (Life Technologies). Sense probes were used as negative controls.

2.7.2. In situ hybridization:

In situ hybridization was performed as described previously (Le Maitre et al., 2013). Briefly, tissue sections were post-fixed in 4% paraformaldehyde and then treated with 0.25% acetic anhydride in 0.1 M triethanolamine (pH 8.0). The sections were then dehydrated in a graded series of alcohol and stored at −20 °C. The sections were prehybridized using 50% (vol/vol) deionized formamide (pH 5.0), 50 mM Tris-HCl (pH 7.6), 25 mM EDTA (pH 8.0), 20 mM NaCl, 0.25 mg/ml, yeast tRNA and 2.5 × Denhardt's solution for 4 h at 55 °C followed by hybridization in a humidified chamber overnight (14–16 h) at 55 °C. The labeled probes were diluted to a final concentration of 1.0 × 106 cpm/200 μl in a solution containing 50% (vol/vol) deionized formamide (pH 5.0), 0.3 M NaCl, 20 mM DTT, 0.5 mg/mL yeast tRNA, 0.1 mg/mL poly-A-RNA, 10% (vol/vol) dextran sulfate, and 1 × Denhardt's solution. After hybridization, sections were washed as follows: twice for 30 min in 1 × SSC at 55 °C, 1 h in 50% (vol/vol) formamide/0.5 × SSC at 55 °C, 15 min in 1 × SSC at 55 °C, 1 h in RNase A buffer at 37 °C, twice for 15 min in 1 × SSC at 55 °C, then were dehydrated in ascending alcohol series (2 min each), and finally were air dried. The sections were exposed to Kodak BioMax MR film (VWR International, Stockholm, Sweden) and then were dipped in Kodak NTB emulsion for autoradiogrpahy (VWR International, Stockholm, Sweden). After a determined exposure time (6 weeks for mouse *Lpar1* and 8 weeks for human *Lpar1*) slides were developed using Kodak D19 developer (VWR International, Stockholm, Sweden) for 3 min and AL4 fixative for 7 min, dried at room temperature (RT, 22 °C) and then mounted with medium containing 90% (vol/vol) glycerol/10% (vol/vol) PBS.

Dark-field pictures of sections processed for *in situ* hybridization were captured on a Nikon microscope equipped with a Coolpix 5000 digital camera (Nikon, Tokyo, Japan). Pictures of silver particle labeling and cresyl violet counterstaining were captured on an Olympus IX73 inverted microscope (Olympus, Tokyo, Japan).

2.8. Conditioned cell culture media analysis

SGC cultures were stimulated for 24 h with 10 μM 18:1 LPA and conditioned culture media was then collected, flash frozen and stored at −80 °C until use. CXCL1, TNF and IL-1β levels in the media were evaluated using an MSD Proinflammatory Panel 1 kit (Mesoscale Discovery Systems, catalogue # K15048D). The assay was performed according to the manufacturer's instructions. Cytokine levels of undiluted media samples were measured in technical duplicates. The plate was read using a MSD QuickPlex SQ 120 (Mesoscale Discovery Systems) and the data were analyzed in Mesoscale Workbench (Mesoscale Discovery Systems).

2.9. Statistics

Mechanical and heat hypersensitivity behavioral data, and quantification data for immunohistochemistry, qPCR and western blotting is presented as mean ± standard error of mean (SEM) and cold hypersensitivity data are presented as the median with the interquartile range. To compare mechanical hypersensitivity a two-way ANOVA for repeated measures with the Geisser-Greenhouse correction in order to not assume sphericity and Tukey's *post-hoc* test was used. Heat and acetone cold sensitivity were assessed by a one-way ANOVA with Tukey's *post hoc* test and SDs were assumed to be equal. Immunohistochemistry and gene expressed data were analyzed by a one-way ANOVA with Tukey's post hoc test and SDs were assumed to be equal. Arthritis clinical scores were assessed at the group level with Kruskal-Wallis test followed by Dunn's post hoc test. An unpaired, two-tailed *t*-test was used

when there were only two groups. Outliers were not removed and a p value<0.05 was considered significant. Data was analyzed with Prism 9.0 (GraphPad Software, La Jolla, CA).

3. Results

3.1. Pain-related behavior is prevented by 504B3

To investigate a potential role for LPA signalling in CAIA-induced pain-like behavior, we injected the monoclonal antibody 504B3, originally developed against LPA, or an isotype matched control monoclonal antibody subcutaneously (s.c., 10 mg/kg) twice weekly beginning 8-days prior to CAIA induction (Fig. 1**A**). Surprisingly, visual signs of joint inflammation developed normally in CAIA mice regardless of antibody treatment ($p > 0.999$, Fig. 1**B**). Ankle joint gene expression of *Il1b, Tnf*, *Ptgs2* and *Ngf* was also not significantly affected by 504B3 ($p > 0.1$, Fig. 1**C**). However, the development of CAIA-induced mechanical hypersensitivity was prevented by pre-treatment with 504B3 (two-way ANOVA: $F(2,12) = 9.852$, $p = 0.0029$; $p < 0.05$ day 10–15, Fig. 1**D**).

3.2. Pain-related behaviors are reversed by 504B3

To examine if established mechanical hypersensitivity is reversed by 504B3, treatment (10 mg/kg, twice weekly) was initiated 12 days after CAIA induction (inflammatory phase) and continued until day 42 (late phase, Fig. 2**A**). Like the pre-treatment study, 504B3 had no effect on CAIA-induced joint inflammation compared to CAIA animals treated with saline or a control antibody ($p = 0.4023$, Fig. 2**B**). In contrast, CAIA-induced mechanical hypersensitivity was gradually reversed by 504B3, reaching levels comparable to saline control mice after 21 days of treatment and lasting throughout day 42, the last day of injection (two-way ANOVA: $F(3,20) = 29.12$, $p < 0.0001$; $p = 0.03$ to 0.0001 day 21–44, Fig. 2**C**). Mechanical hypersensitivity in CAIA mice re-developed following the end of antibody treatment (Fig. 2**C**). A lower dose of 504B3 (2 mg/kg) had no effect on inflammation ($p = 0.443$) or mechanical hypersensitivity (two-way ANOVA: $F(3, 220) = 39.02$, $p < 0.0001$; $p > 0.3$ comparing CAIA with control antibody vs 504B3, **Supp.** Fig. 1). Therefore, only 10 mg/kg of 504B3 was used for the remainder of the study.

To test if temperature hypersensitivity is also reversed by 504B3, cold allodynia was assessed with the acetone test and heat hypersensitivity was examined using a modification of the Hargreaves test. CAIA-induced cold ($p = 0.0014$, Fig. 2**D**) and heat hypersensitivity ($p = 0.0057$, Fig. 2**E**) were both reversed by 504B3 during the inflammatory phase. During the late, neuropathic-like phase of CAIA, heat hypersensitivity was not significantly elevated comparing saline treated and CAIA animals treated with saline, but 504B3 did significantly reduce CAIA-induced heat hypersensitivity compared to control antibody treated animals ($p = 0.0435$, Fig. 2**E**). Cold hypersensitivity was not significantly elevated in CAIA animals compared to saline treated animals (Fig. 2**D**).

We also examined if CAIA pain-like behavior would be reversed when beginning treatment with 504B3 in the late, neuropathic-like phase (day 57). A 14-day drug washout period was initiated at day 42, during which the withdrawal thresholds dropped in the 504B3/CAIA group, reaching the same level of mechanical hypersensitivity as in the control antibody treated CAIA group (Fig. 2**C**). We then employed a cross over design. From day 57 i) CAIA mice that had previously received saline were switched to 504B3, ii) CAIA mice that had previously received 504B3 were switched to control antibody, iii) CAIA mice that had received the control antibody were switched to saline and iv) control mice continued to received saline. Mice were treated twice per

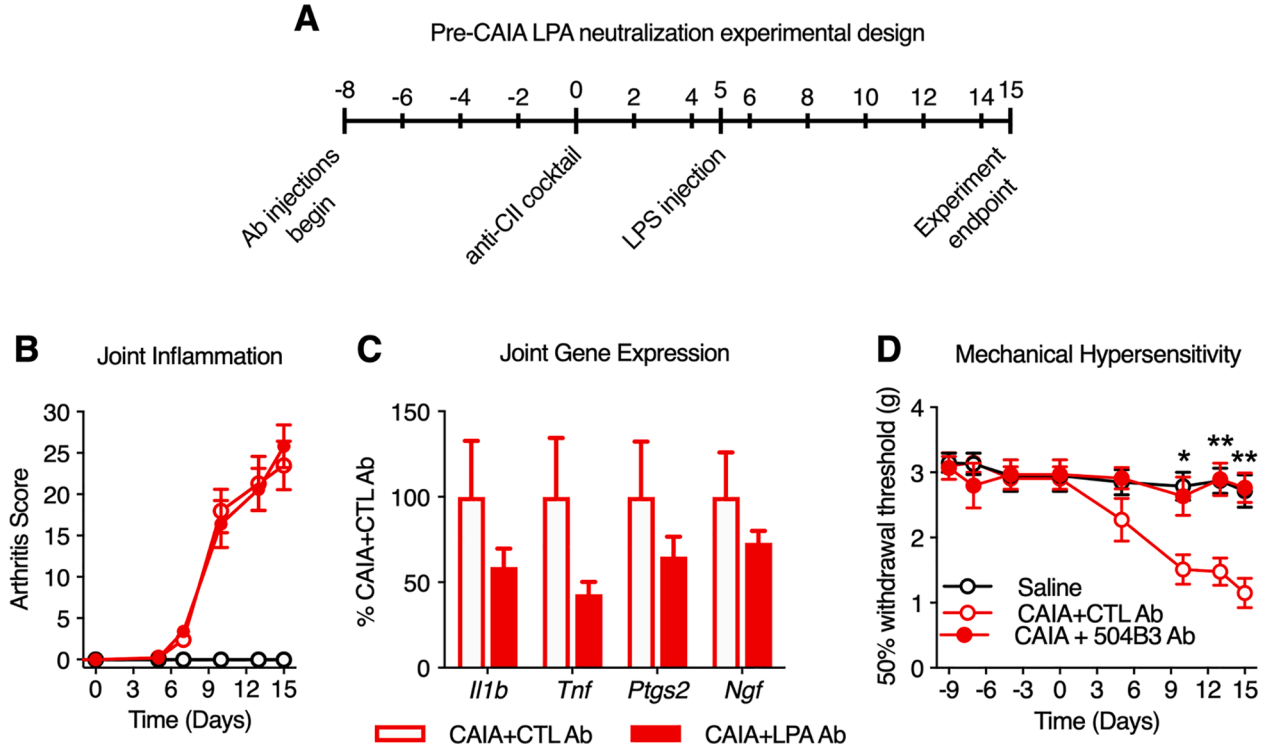

Fig. 1. CAIA-induced pain-like behavior is prevented by 504B3. (**A**) Beginning eight days prior to CAIA induction, mice received a neutralizing monoclonal antibody generated against LPA (504B3 Ab,10 mg/kg), a control antibody (CTL Ab, 10 mg/kg) or saline subcutaneously twice weekly, n = 5/group. (**B**) Joint inflammation was assessed by visually determining the arthritis score. (**C**) Inflammatory and nociceptive ankle joint gene expression was assessed and data was analyzed using the relative standard curve method. (**D**) Mechanical sensitivity was evaluated with von Frey testing. Mechanical hypersensitivity data was analyzed by repeated measures two-way ANOVA with a Tukey's post-hoc test and gene expression data was analyzed by two-tailed t-tests. Data are presented as mean ± SEM. *indicates $p < 0.05$, ** indicates $p < 0.01$, *** indicates $p < 0.0001$ when comparing CAIA + 504B3 Ab with CAIA + CTL Ab.

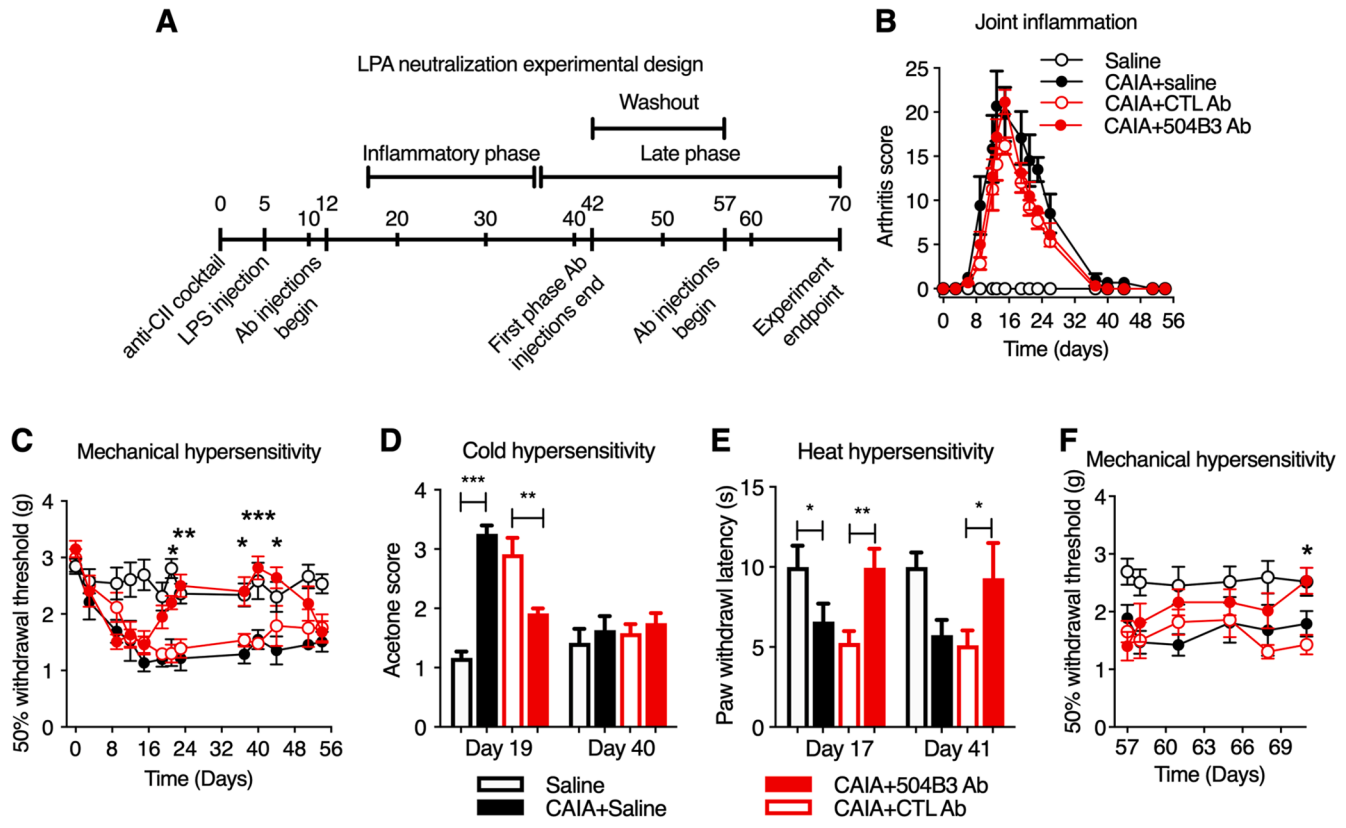

Fig. 2. CAIA-induced pain-like behavior is reversed by 504B3. (**A**) 12 days after CAIA induction, the neutralizing antibody, the control antibody or saline were delivered subcutaneously twice weekly until day 42. Following a 14-day washout period treatment groups were reassigned and the neutralizing antibody, the control antibody or saline were delivered subcutaneously twice weekly from day 57 until day 70, n = 6/group. (**B**) Joint inflammation was assessed by visually scoring the severity of arthritis characteristics in the paws and (**C**) mechanical hypersensitivity was quantified during the first treatment phase of the experiment. (**D**) Cold hypersensitivity was assessed by quantifying acetone evoked behavior using a scoring system. (**E**) Heat hypersensitivity was evaluated using a Hargreaves-type device and the time to paw withdrawal following application of a heat stimuli was quantified. (**F**) Mechanical hypersensitivity was assessed following the treatment group crossover during the second treatment phase of the experiment. Mechanical hypersensitivity data was analyzed by repeated measures two-way ANOVA with Tukey's post-hoc test, heat and cold hypersensitivity were assessed by one-way ANOVA with a Tukey's post-hoc test. Joint inflammation, mechanical hypersensitivity and heat hypersensitivity are presented as mean ± SEM. Cold hypersensitivity data is ordinal and is therefore presented as median ± interquartile range. *indicates $p < 0.05$, ** indicates $p < 0.01$, *** indicates $p < 0.0001$ when comparing CAIA + 504B3 Ab with CAIA + CTL Ab.

week. When compared to CAIA control mice, mechanical hypersensitivity was gradually reversed by the antibody (two-way ANOVA: $F = 12.69$, $p < 0.0001$; $p = 0.0149$ day 71, Fig. 2**F**). Taken together, these results suggest that sequestering LPA during the inflammatory phase (starting either before or during ongoing joint inflammation) or following joint inflammation is sufficient to reduce CAIA-induced pain-like behavior.

3.3. $LPA_{1/3}$ inhibition reduces CAIA-induced mechanical hypersensitivity

To further examine if LPA contributes to CAIA-induced hypersensitivity we used Ki-16425, an antagonist of LPA_1 and LPA_3 (K_i values 250 nM and 360 nM, respectively). Ki-16525 was delivered daily beginning 14 days after CAIA induction (Fig. 3**A**). $LPA_{1/3}$ antagonism gradually reversed CAIA-induced mechanical hypersensitivity compared to vehicle treated mice (two-way ANOVA: $F(2,18) = 28.41$, $p < 0.0001$; $p = 0.0239$, Fig. 3**B**). While $LPA_{1/3}$ inhibition did not reduce the magnitude of joint inflammation, the inflammation resolved at an earlier time point (35 days) compared to vehicle treated CAIA mice (two-way ANOVA: $F(2,17) = 10.19$, $p = 0.0012$; $p = 0.0396$, Fig. 3**C**). Thus, LPA signalling may regulate CAIA-induced pain-like behavior via LPA_1 or LPA $_3$. Furthermore, these results suggest that the anti-nociceptive effects of 504B3 are at least partly due to preventing the actions of 18:1 LPA.

3.4. Intraarticular ankle joint injection of 18:1 LPA does not induce pain-like behavior

In other studies in rats, a role for LPA signalling in RA joint inflammation has been suggested (Miyabe et al., 2013; Nikitopoulou et al., 2012; Orosa et al., 2012) and intraarticular knee injection of LPA induced mechanical hypersensitivity in rats (O'Brien et al., 2018). We therefore examined whether intra-articular ankle joint injection of LPA induces pain-like behavior over seven days. 18:1 LPA did not alter mechanical withdrawal thresholds compared to vehicle injected mice two or six hours after injection ($F(3, 20) = 0.1759$, $p = 0.9114$, Fig. 4**A**) nor at one, three or seven days ($F(5, 36) = 1.307$, $p = 0.283$, Fig. 4**B**). This finding combined with the lack of reduction of joint inflammation with the antibody and $LPA_{1/3}$ inhibition indicates that the joint may not be the primary site where LPA is exerting pronociceptive effects in the CAIA model.

3.5. Autotaxin is upregulated and LPA receptors are expressed in the DRG

Since blocking LPA signalling does not reduce ankle inflammation and intraarticular ankle joint injection of 18:1 LPA did not induce pain-like behavior, we next investigated if LPA is modulating neuronal excitability at the level of the DRG soma during CAIA. We analyzed the expression of *Enpp2,* the gene encoding autotaxin (ATX), which is an enzyme that converts LPC to LPA (Tokumura et al., 2002). In the DRG

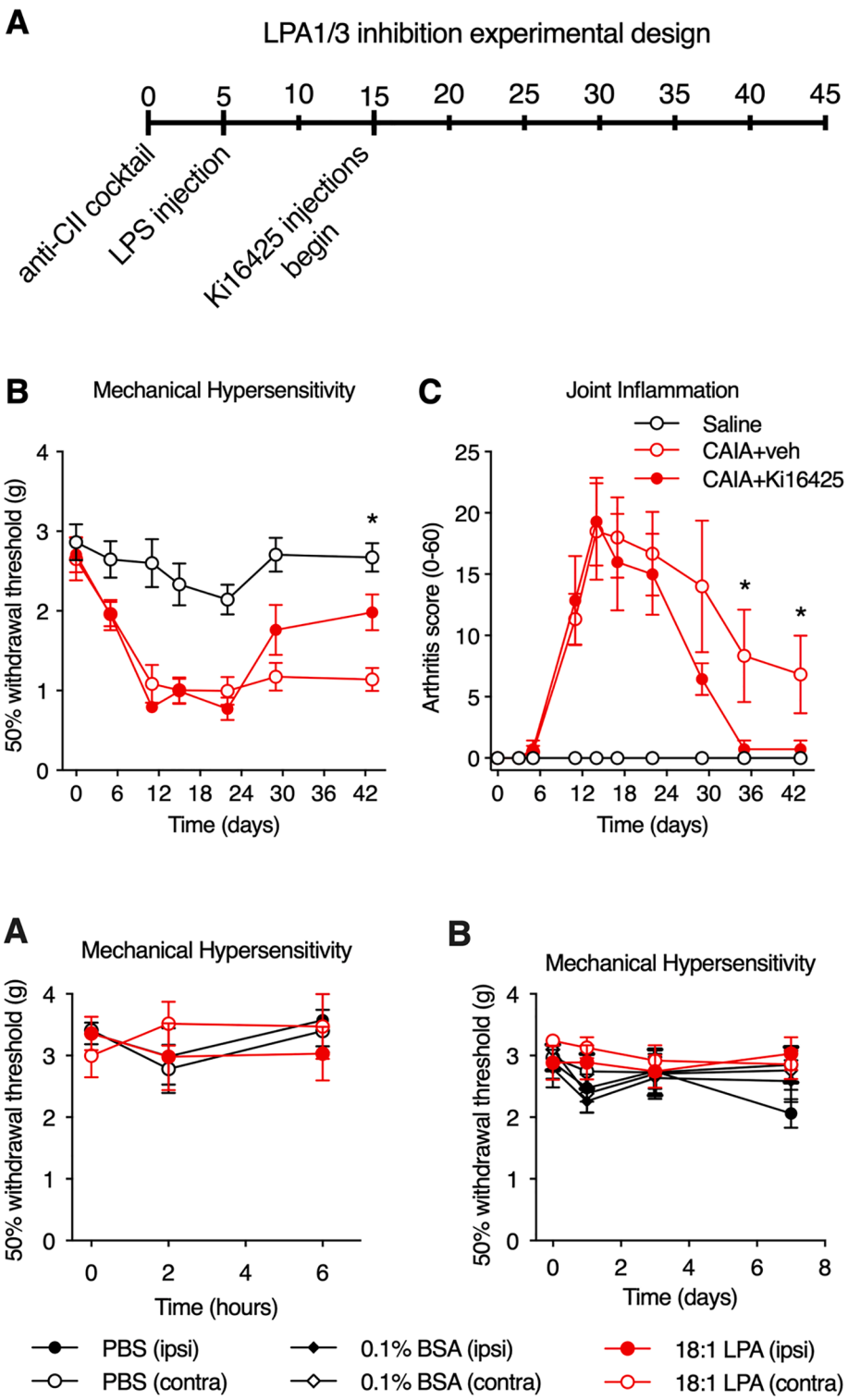

Fig. 3. Inhibition of LPA_1 and LPA_3 signalling decreases CAIA-induced mechanical hypersensitivity. (**A**) Ki-16425 injections began 15 days after CAIA induction. (**B**) Visual signs of join inflammation were assessed by arthritis scoring in saline treated mice, CAIA mice that received vehicle treatment (CAIA + veh) and CAIA mice that received Ki-16425 (CAIA + Ki-16425). (**C**) Mechanical hypersensitivity was analysed by von Frey testing. Data are presented as mean ± SEM and was analyzed by repeated measures two-way ANOVA with Tukey's post-hoc test, n = 6–8/group, * indicates $p < 0.05$ when comparing CAIA + Ki-16425 treated mice with CAIA + veh treated mice.

Fig. 4. Intraarticular ankle joint LPA injection does not induce mechanical hypersensitivity. 18:1 LPA (250 pmol in 5 µl PBS with 0.1% BSA), PBS or vehicle were injected intraarticularly and mechanical hypersensitivity was tested in the injected, ipsilateral paw and the contralateral paw. (**A**) The acute effect of 18:1 LPA was evaluated over six hours and (**B**) in a separate experiment the long-term effect of 18:1 LPA was evaluated over seven days. Data were analyzed by repeated measures two-way ANOVA with Tukey's post-hoc test. Data are presented as mean ± SEM, n = 7 per group.

Enpp2 is significantly increased in the inflammatory phase of CAIA ($p = 0.0198$), and the late phase ($p = 0.042$, Fig. 5**A**). In contrast, *Enpp2* expression is not elevated in the spinal cord during either phase of CAIA ($p = 0.397$ or 0.656, Fig. 5**B**) nor in the ankle joint during the inflammatory phase of CAIA ($p = 0.81$, Fig. 5**C**). We then examined ATX protein levels and found that an increased percentage of DRG neurons were ATX-immunoreactive during the inflammatory ($p = 0.046$, Fig. 5**D, E**) and the late phase ($p < 0.001$, Fig. 5**F, G**) of CAIA compared to control mice.

LPA acts as a ligand for at least six GPCRs, $LPA_{1\text{-}6}$ (Choi et al., 2010; Kihara et al., 2014; Yung et al., 2014). Using qPCR, we confirmed that *Lpar1-6* mRNA transcripts are present in DRGs. While *Lpar1*, *5* and *6* expression levels were higher than *Lpar2, 3* and *4* (Fig. 5**H**), the expression levels of the six receptors did not change during the inflammatory phase (p's > 0.43, Fig. 5**I**) or the late phase (p's > 0.15, Fig. 5**J**) of CAIA when compared to controls. Expression of spinal *Lpar1*, which is expressed by microglia, is also unaltered during the inflammatory and late phases of CAIA (**Supp** Fig. 2**A, B**). Taken together, these

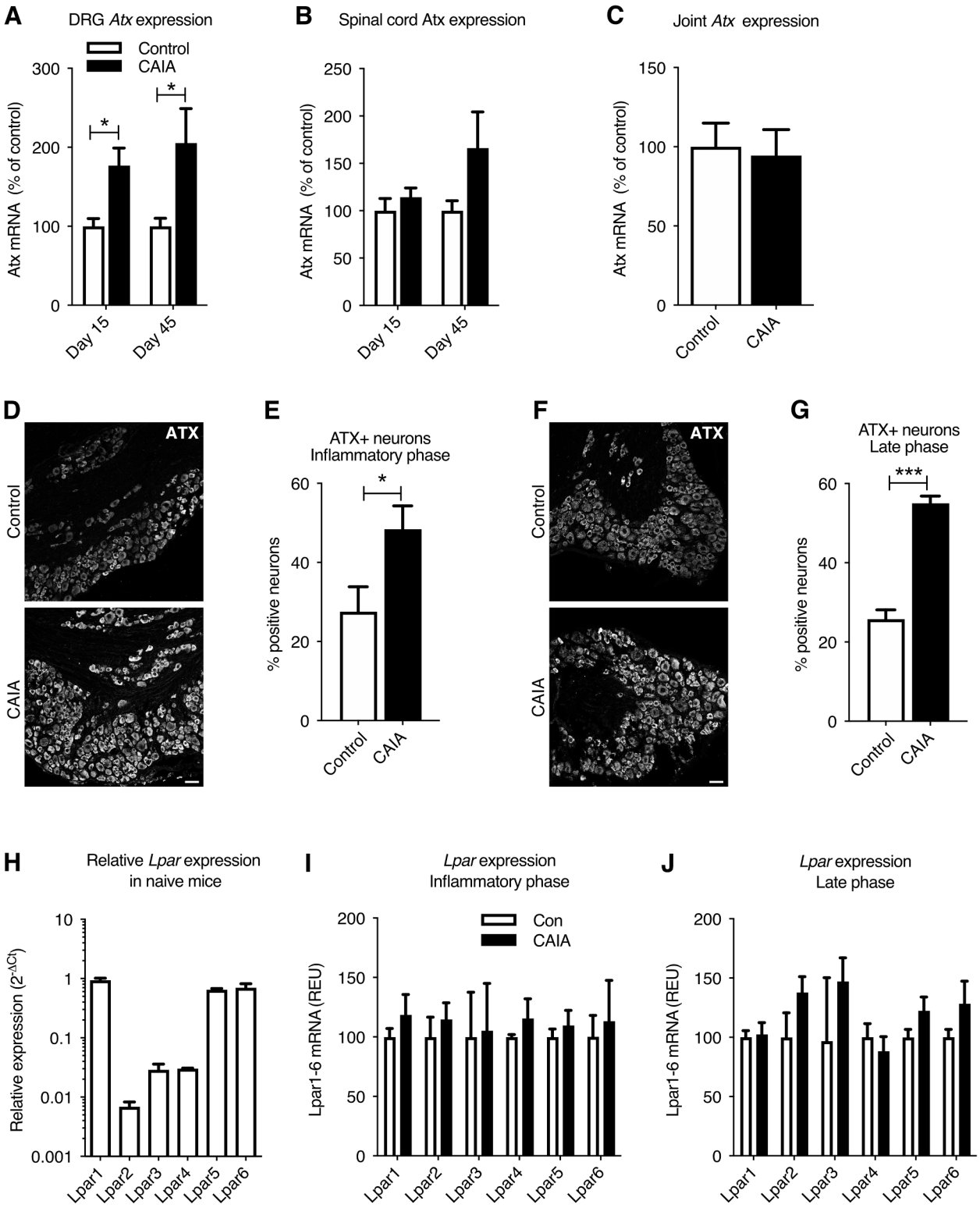

Fig. 5. Signs of elevated LPA signalling in the dorsal root ganglia (DRG) (**A**) *Autotaxin* (*ATX*) gene expression in the lumbar DRGs, (**B**) the lumbar spinal cord and (**C**) the ankle joint was analyzed with qPCR during the inflammatory phase (Day 15) and late phase (Day 45, DRGs and spinal cord only) of CAIA and control mice. Data are normalized to saline treated animals using the standard curve method. (**D**, **F**) Representative images of autotaxin (ATX) immunoreactivity in DRGs and (**E, G**) quantification of ATX-immunoreactive neurons from the inflammatory (**D, E**) and late phase (**F, G**) of CAIA and control mice. Scale bar indicates 50 μm. (**H**) The relative expression levels of *Lpar1-6* was assessed with qPCR and data was normalized against *Hprt1* using the $2^{-\Delta Ct}$ method. The effect of CAIA on the gene expression of *Lpar1-6* was analyzed in the DRGs during the (**I**) inflammatory and (**J**) late phase of CAIA with qPCR. Data were normalized to expression levels in saline treated animals using the standard curve method. Data were analyzed by t-tests, n = 4–6/group, *indicates $p < 0.05$, *** indicates $p < 0.001$ when comparing CAIA and control mice.

findings demonstrate that the necessary components for LPA signalling are present in the DRG and that LPA levels may locally increase.

3.6. 18:1 LPA increases pain-related ion channels and galanin in DRG cultures

ATX can convert LPC to LPA species. We examined if exposure to 18:1 LPA, 18:2 LPA or 18:1 cyclic LPA altered the voltage-gated calcium channel (VGCC) α2δ1subunit protein expression in dissociated DRG cultures and found that only 18:1 LPA transiently increased α2δ1 protein levels compared to vehicle ($p < 0.001$, Fig. 6**A-C**). We also assessed the gene expression of *Cacna2d1* (α2δ1 gene), *P2rx3* (P2X3 gene) and *Gal* (galain gene) following 18:1 LPA stimulation and found that like the western blot results, *Cacna2d1* expression increased after 4 h compared to vehicle ($p = 0.0042$), before returning to control levels (Fig. 6**D**). *P2rx3* expression significantly increased after 4 h of treatment compared to control ($p = 0.0042$, Fig. 6**E**) while *Gal* expression significantly increased after 24 h of stimulation compared to control ($p = 0.0042$, Fig. 6**F**). Immunofluorescence staining of primary DRG neurons showed that an increased percent of neurons expressed α2δ1 following 18:1 LPA treatment compared to vehicle ($p < 0.001$, Fig. 6**G, H**). These results indicate that 18:1 LPA stimulation of DRG cultures increases pain-related ion channels and galanin in neurons.

3.7. LPA_1 is present on satellite glial cells

As 18:1 LPA has higher affinity for LPA_1 than LPA_3 ($EC_{50} \sim 10$ nM for LPA_1 and $EC_{50} \sim 100$ nM for LPA_3) (Bandoh et al., 2000; Kano et al., 2019; Yung et al., 2014), and only 18:1 LPA caused a response in DRG cultures, we focused on LPA_1. In mouse and human DRGs *Lpar1 in situ* hybridization showed that transcripts are primarily located in a pattern around neuronal soma, with few transcripts in the soma, suggesting non-neuronal expression (Fig. 7**A, B**). Control experiments with sense probes showed no specific localization patterns (**Supp.** Fig. 3). Similarly, immunofluorescence indicated a non-neuronal expression of LPA_1, with LPA_1 immunoreactivity forming a circular staining pattern around α2δ1-positive neuronal soma in both human and mouse DRG neurons (Fig. 7**C-F**). Critically, LPA_1 immunoreactivity was absent in *Lpar1-/-* mice (Fig. 7**C**). Thus, both *in situ* hybridization and immunofluorescence staining profiles suggest that LPA_1 is expressed by satellite glial cells (SGCs) in the DRG. To determine the cellular localization of LPA_1, we examined if LPA_1 colocalizes with glutamine synthase (GS) and/or Iba1, markers for SGCs and DRG resident macrophages, respectively. LPA_1 immunoreactive cells co-localized with GS (Fig. 7**G)** but not Iba1 immunoreactivity (Fig. 7**H**). Taken together, these data demonstrate that SGCs express LPA_1 in the DRG.

3.8. Satellite glial cells are activated by LPA

SGCs modulate neuronal activity and morphological signs of increased SGC activity have been reported in a number of pain models (Ji et al., 2013; Ohara et al., 2009). Therefore, we examined if CAIA induces changes in glial fibrillary acidic protein (GFAP) expression, which is used as a marker of enhanced SGC activity (Ohara et al., 2009). During the inflammatory phase of CAIA (day 16), the % area of GFAP immunoreactivity ($p < 0.001$) and GFAP pixel intensity ($p < 0.001$) in DRGs from mice subjected to CAIA (and control antibody) were increased compared to saline injected control mice. Injection of 504B3 decreased GFAP-ir compared to CAIA mice that received the control antibody ($p = 0.0144$ or $p = 0.0072$, Fig. 8**A - C**). Furthermore, development of CAIA driven % area of GFAP immunoreactivity ($p = 0.001$) and GFAP pixel intensity ($p = 0.005$) increases are blocked in *Lpar1* deficient mice compared to wild-type (Fig. 8**D-E**).

To confirm a direct effect of LPA on SGCs, SGC-enriched cultures were exposed to 18:1 LPA for 4 h, which resulted in increased *Gfap* mRNA expression compared to vehicle SGC cultures ($p = 0.048$, Fig. 8**G**). Gene expression of the pronociceptive cytokines, *Il1b* ($p = 0.0222$), *Il6* ($p = 0.0493$), *and Tnf* ($p = 0.046$), and *Ngf* ($p = 0.0024$) were increased in response to 18:1 LPA compared to vehicle treated cells (Fig. 8**H)**. We also stimulated SGCs for 24 h and assessed protein release in culture medium. 18:1 LPA increased CXCL1 ($p = 0.0127$) levels, while TNF levels showed a trend of increased secretion ($p = 0.0503$) and IL-1β was unchanged compared to vehicle treated cells (Fig. 8**I -J**). In sum, 18:1 LPA can directly act on SGCs to increase pronociceptive factors and LPA neutralization decreases signs of CAIA induced SGC activity.

3.9. LPA_1 signalling regulates DRG pain-related protein expression

We examined expression of the VGCC α2δ1 subunit in DRG by immunohistochemistry as the number of α2δ1positive neurons and intensity of α2δ1 immunoreactivity in the late-phase (day 47) of CAIA model. We confirmed our previous finding that CAIA generates an increase in both parameters when compared to saline treated mice ($p < 0.001$, Fig. 9**A-C**). 504B3 treatment normalized α2δ1 expression to levels similar to control mice ($p < 0.001$ or $p = 0.0166$, Fig. 9**A-C**). In *Lpar1-/-* mice α2δ1 expression is similar to wild type mice (Inoue et al., 2004). We found that *Lpar1-/-* mice are protected from CAIA-induced α2δ1 increases compared to WT CAIA mice 47 days after induction ($p < 0.001$ and $p = 0.0019$, Fig. 9**D-F**). These results suggest that LPA, via activation of LPA_1 in SGCs, regulate neuronal α2δ1 expression in the late-phase of CAIA. In a similar fashion, galanin and P2X3 expression assessed by immunohistochemistry, are also increased in DRG of CAIA mice compared to controls ($p < 0.001$) (Su et al., 2015) and blocking the availability of LPA or its precursors reduced the increase of these two factors to similar levels as in control mice ($p < 0.001$, Fig. 9**G-J**). Spinal microglia, which express LPA_1, displayed increased Iba1 immunoreactivity in CAIA late phase ($p = 0.0291$, but systemic treatment with 503B4 did not reduce the morphological signs of enhanced microglia reactivity ($p > 0.999$, **Supp.** Fig. 2**C, D**). Taken together, these results suggest that inhibition of LPA signalling reduces SGC-neuronal communication, normalizing CAIA-induced changes of pain-related proteins.

4. Discussion

In the current study we describe how LPA-LPA_1 signalling drives pain-like behavior in CAIA via SGCs by a mechanism that is independent of inflammation. First, we found that neuronal ATX, an LPA producing enzyme, was elevated in the DRG. Second, CAIA-induced pain-like behavior during the inflammatory and/or late phases of the model was attenuated by a monoclonal LPA-binding antibody (504B3) and a $LPA_{1/3}$ antagonist. In dissociated primary DRG cultures, stimulation with 18:1 LPA increased gene and protein expression of α2δ1. Third, we detected protein expression of LPA_1 only on SGCs in both human and mouse DRGs. 18:1 LPA also increased signs of SGC activity and pronociceptive cytokine expression *in vitro*. Similarly, CAIA increased signs of SGC activity *in vivo*, which was reversed by 504B3 treatment and in *Lpar1* deficient mice. Lastly, CAIA-induced α2δ1, P2X3 and galanin expression was reduced by *Lpar1* deficiency and 504B3. Taken together, our results indicate that ATX-LPA-LPA_1 signalling is a contributing pronociceptive mechanism in CAIA and that it initiates neuron-to-SGC-to-nociceptor communication that regulates expression of factors critical for long-lasting pain-like behavior (Fig. 10).

Previous studies have linked LPA-driven demyelination to pain. In those studies, pre-treatment paradigms or genetic approaches, which are akin to pre-treatment, were primarily used to block either LPA_1, LPA_3 or ATX activity. LPA_1 or LPA_3 receptor inhibition, LPA_1 deletion ($Lpar1^{-/-}$ mice) or heterozygous *Enpp2* (*Enpp2*$^{+/-}$) expression prevented or reduced demyelination following sciatic nerve injury, monoiodoacetate-induced arthritis, and LPA injection (Inoue et al., 2008, 2004; McDougall et al., 2017; Nagai et al., 2010). However, there is limited information about whether inhibiting LPA signalling reverses demyelination.

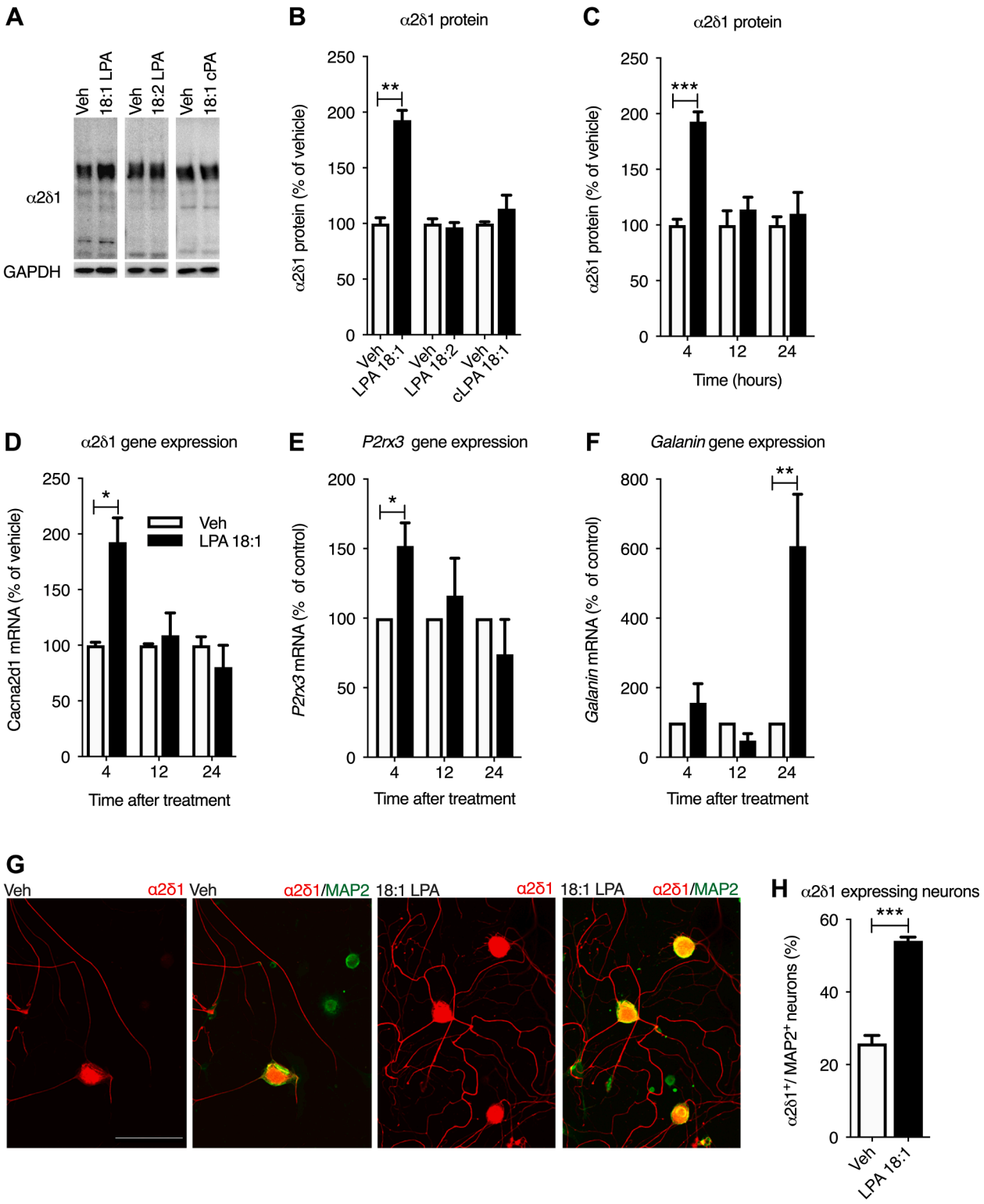

Fig. 6. 18:1 LPA increases α2δ1, P2X3 and Galanin expression. Dissociated DRG cultures were treated with 18:1 LPA, 18:2 LPA and 18:1 cPA. Cultures were then either lysed for protein or RNA extraction or fixed for immunofluorescence. (**A**) Representative images of western blots probed for α2δ1 following four hours of 18:1 LPA, 18:2 LPA or 18:1 cLPA treatment and the GAPDH loading control. (**B**) α2δ1 levels were quantified by densitometric analysis, normalized to GAPDH and presented as the % of α2δ1 in vehicle treated cell cultures. (**C**) α2δ1 protein levels were also quantified after 4, 12 and 24 h of 18:1 LPA treatment. Gene expression levels of (**D**) *Cacna2d1*, (**E**) *P2x3* and (**F**) *Galanin* were assessed with qPCR after 4, 12 and 24 h. Expression levels were normalized to *Hprt1* and analyzed using the standard curve method. (**G**) DRG cultures treated with vehicle or 18:1 LPA were stained with antibodies against α2δ1 (red) or MAP2 (green), a general neuronal marker and (**H**) the present of neurons expressing α2δ1 was calculated. Data is presented as mean ± SEM and assessed with two-tailed t-tests, n = 3–4/group, * indicates $p < 0.05$, ** indicates $p < 0.001$ when comparing LPA treated cells with vehicle treated cells. (For interpretation of the references to colour in this figure legend, the reader is referred to the web version of this article.)

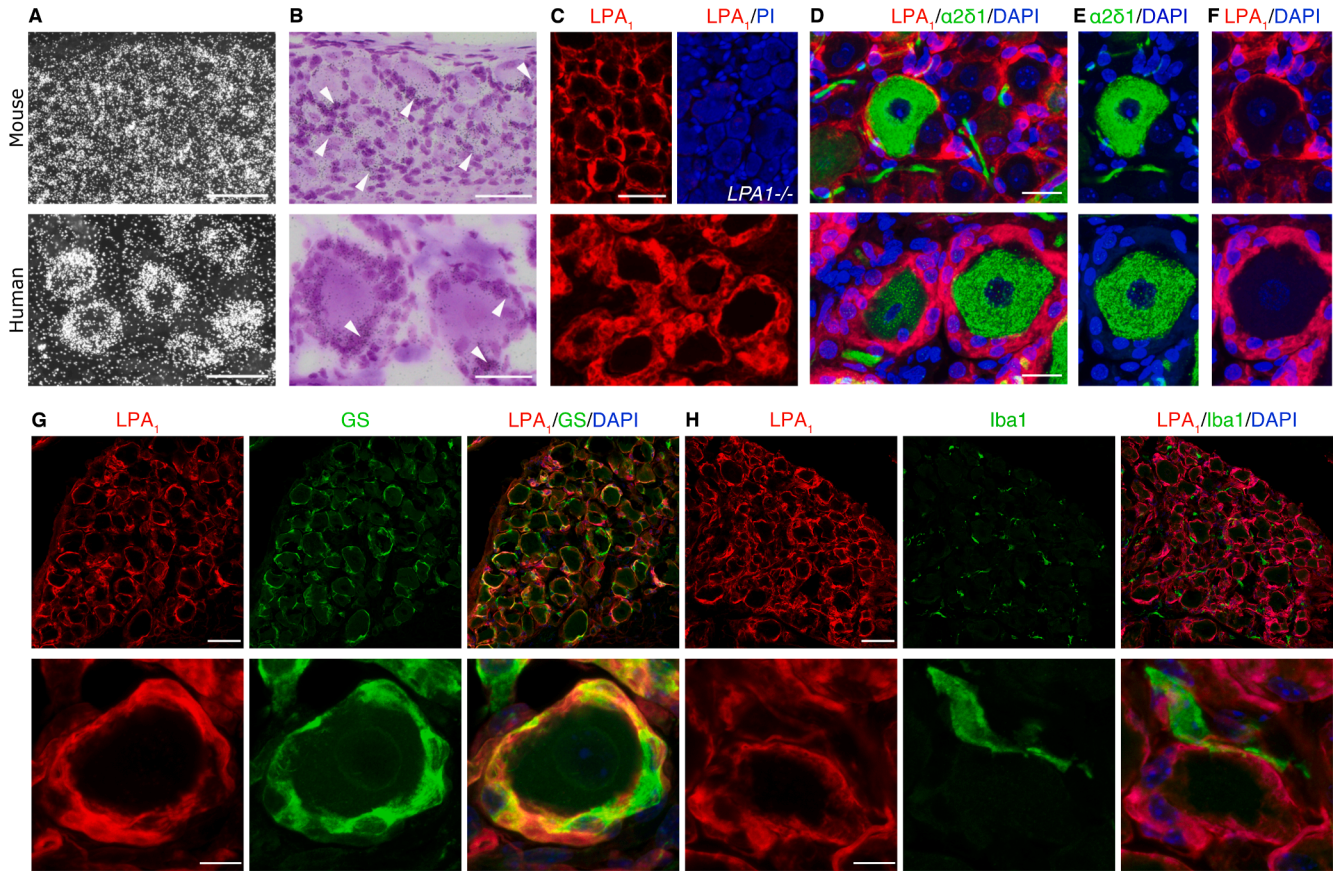

Fig. 7. Satellite glia cells (SGCs) express LPA_1. (**A-F**) Mouse (top row) and human (bottom row) expression of LPA_1 was assessed with a number of techniques. (**A**) *In situ* hybridization analysis shows patch-like signals in mouse at low power (dark field) and (**B**) high-power bright field (cresyl violet) image reveals *Lpar1* expression in cells surrounding DRG neurons. (**C**) DRGs from wild-type mice, *Lpar1*$^{-/-}$ mice and a human organ donor were probed for LPA_1. (**D-E**) LPA_1 (red) expressing cells surround numerous sizes of neurons including those that express α2δ1 (green). (**G**) LPA_1 (red) is expressed by glutamine synthase (GS, green), (**H**) but not Iba1(green) expressing cells. Scale bars: 100 μm in **A**; 50 μm in **B, C, G** (top row), **H** (top row); 20 μm in **D**, **G** (bottom row), **H** (bottom row). (For interpretation of the references to colour in this figure legend, the reader is referred to the web version of this article.)

Paradoxically, LPA receptor signalling also has documented physiological roles in myelinating cells during nervous system development (Weiner et al., 2001, 1998; Weiner and Chun, 1999). We did not investigate nerve demyelination in the current study, and though it cannot be excluded, it seems unlikely that the reduction of pain-like behavior we observed in as little as five days is due to a recovery of myelin. Here we suggest an additional peripheral mechanism by which local DRG LPA signalling drives neuropathic-like pain via SGC activation in CAIA. In agreement with our observation, a recent study using calcium imaging showed that 18:1 LPA stimulates SGCs *in vitro* (Robering et al., 2019). Unlike pre-treatment paradigms, our results from post-treatment experiments demonstrate that blocking LPA signalling can reverse inflammatory and neuropathic pain-like behavior.

Our *in vitro* and *in vivo* pharmacological and genetic studies suggest that LPA_1 is the main LPA receptor driving nociceptive-associated changes in the DRG via SGCs. We found *Lpar1* mRNA and LPA_1 protein only in SGCs and not in DRG neurons or resident macrophages in both mouse and human DRGs. This finding is further supported by single cell RNA sequencing (scRNA-seq) demonstrating *Lpar1* mRNA, but not *Lpar3* is expressed in mouse SGCs (Zeisel et al., 2018) and single nucleus RNA-seq of human DRG neurons showing little to no LPAR1 expression in neurons (Nguyen et al., 2021). A recent study also reported that LPA_1 protein is exclusively expressed in SGCs in rats and mice (Robering et al., 2019). Moreover, LPA does not activate sensory neurons *in vitro* (Robering et al., 2019) and *intraarticular* LPA does not induce mechanical hypersensitivity, suggesting that LPA does not directly stimulate nociceptors.

LPA receptors and autotaxin are widely expressed in neuronal and non-neuronal cells across the central nervous system in rodents (Fotopoulou et al., 2010; Ma et al., 2010a, 2010b; Savaskan et al., 2007; Zeisel et al., 2018) and in the human cerebral cortex (Palmer et al., 2021). Additionally, the neurological deficits of *Lpar1* deficient mice indicate important developmental and physiological roles of LPA signalling in the brain (Contos et al., 2000; Harrison et al., 2003). However, our data suggests that the reduction of CAIA-induced pain-like behaviour stems at least partly from interference with peripheral LPA signalling. CAIA ATX gene and protein levels were elevated in the DRG, but gene expression was unchanged in the spinal cord or ankle joint, which suggests LPA increases locally in the DRG. ATX in control murine DRG neurons is much lower compared to CAIA and ENPP2 expression in human DRG neurons is low to undetectable with single nucleus RNA-seq (Nguyen et al., 2021), indicating that nociception-associated sensory neuron ATX is inducible. Further supporting a peripheral role for LPA signalling in pain is our finding that CAIA-induced reactivity of microglia, which express LPA_1 (Ma et al., 2010a, 2010b), was unaffected by 504B3. Moreover, Ki-16425 has poor central nervous system penetrance (Sánchez-Marín et al., 2018) and antibody drugs like 504B3 typically do not cross the blood–brain barrier. Thus, our findings do not suggest that the primary effect of LPA-driven pain in CAIA is the central nervous system nor the inflamed ankle joint. Instead, consistent with neuropathic pain models employing conditional LPA_1 removal from SGCs (Rivera et al., 2020), we propose that LPA regulates CAIA-induced pain-like behavior by activating SGCs via LPA_1 in the DRG, which in turn modulates nociceptor sensitivity via changes at the level of the neuronal

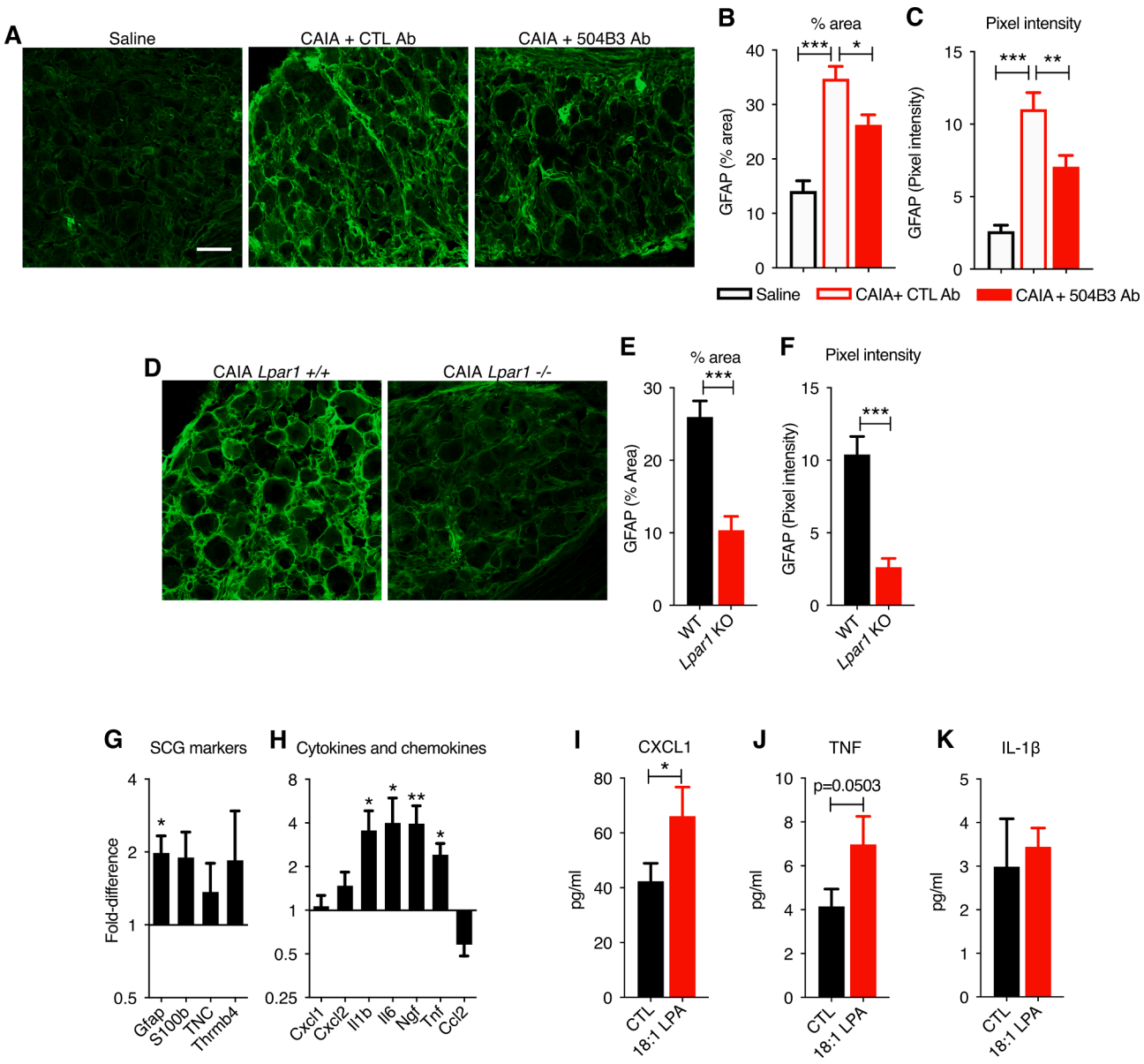

Fig. 8. Satellite cell activity is increased by LPA. SGCs elevate GFAP during increased activity. (**A**) Representative images of GFAP expression in DRGs that were collected 15 days after CAIA induction from mice treated with saline, or CAIA mice treated with the control antibody (CAIA + CTL Ab) or 504B3 (CAIA + 504B3 Ab), the neutralizing antibody generated against LPA. (**B**) The percentage of the neuron-rich DRG area that was GFAP-immunoreactive (% area) and (**C**) the pixel intensity of GFAP were quantified, n = 6/group. **(D)** Representative images of GFAP expression in DRGs from wild-type or *Lpar1* deficient mice with CAIA. **(E)** The % area of GFAP-immunoreactivity and **(F)** pixel intensity of GFAP in the neuron rich region of the DRGs was quantified, n = 4–6. SGC-enriched cultures were treated with 18:1 LPA and gene expression of (**G**) pain-related factors and (**H**) SGC activity markers was evaluated after 4 h. (**I-J**) secretion of proinflammatory and pronociceptive factors were evaluated after 24 h of LPA stimulation. The change in gene expression was calculated as a fold-difference from vehicle treated cultures using the $2^{-\Delta\Delta Ct}$ method with *Hprt1* as the house keeping gene, n = 5. Data is presented as mean ± SEM and was analyzed by one-way ANOVA with Tukey's post-hoc test or a two-tailed *t*-test. * indicates $p < 0.05$, ** indicates $p < 0.01$, *** indicates $p < 0.001$when making the indicated comparisons (GFAP-immunoreactivity) or when comparing 18:1 LPA treated SGCs with vehicle treated SGCs.

soma.

Prior studies have focused on how LPA mediates neuropathic pain, and our results suggest that LPA may also drive inflammatory pain, consistent with published data (Srikanth et al., 2018). However, prior studies assessing changes in neuropathic pain-related factors (e.g. galanin, activating transcription factor 3 and growth-associated protein 43) and pharmacological studies with gabapentin and diclofenac indicate that inflammatory and neuropathic components contribute to pain-like behavior during the inflammatory phase of CAIA (Bas et al., 2012; Su et al., 2015). Studies with inflammatory pain models less complex than CAIA, such as intraarticular CFA or carrageenan, are needed to definitively elucidate whether peripheral LPA signal is a mediator of inflammatory pain.

The pharmacological tools used in this study for interference with LPA signalling have certain limitations. Ki-16425 inhibits LPA_1 and LPA_3, with a slightly lower Ki value for LPA_1 than LPA_3 (250 nM vs 350 nM), thus effects of this drug could be due to antagonism of either receptor. It is notable that actual K_D affinities may be higher than estimated by EC50s, with sub-to-single-digit nanomolar values reported for LPA_1 (Mizuno et al., 2019; Ray et al., 2020), which has relevance for local receptor interactions and LPA concentrations. Nevertheless, *in vitro* culture experiments, qPCR data, single-cell RNA-seq data (Zeisel et al., 2018) and results from *Lpar1*$^{-/-}$ mice all suggest that LPA_1, and not LPA_3, is the major LPA receptor responsible for the LPA-associated findings in

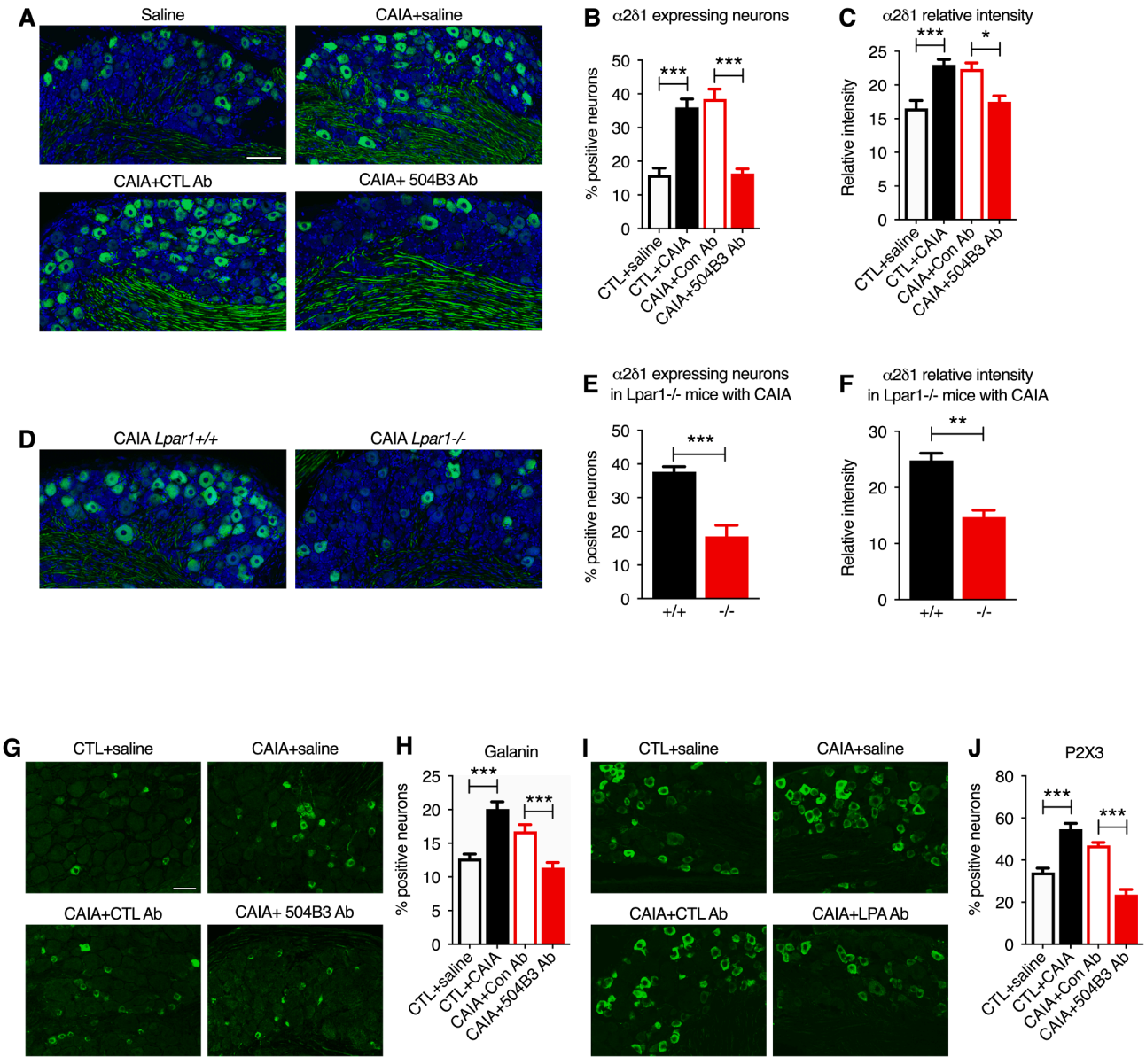

Fig. 9. CAIA driven elevation of nociception-associated DRG proteins is reversed by blocking LPA_1 signalling and 504B3. DRGs from saline treated mice and from CAIA mice receiving saline, the neutralizing antibody generated against LPA (CAIA + 504B3 Ab) or the control antibody (CAIA + CTL Ab) were collected 48 days after CAIA induction. (**A**) DRGs were then probed for α2δ1 immunoreactivity and (**B**) percentage of neurons expressing α2δ1 and (**C**) the relative intensity of α2δ1 immunofluorescence were quantified. CAIA was also induced in *Lpar1*$^{-/-}$ mice and (**D**) α2δ1 immunoreactivity in DRGs was assessed by (**E**) the percentage of neurons expressing α2δ1 and (**F**) relative intensity. (**G**) DRGs were also probed for Galanin immunoreactivity and (**H**) percentage of neurons expressing Galanin cells was quantified. (**I**) Similarly, P2X3 immunoreactivity was probed and (**J**) the percentage of neurons expressing P2X3 was quantified. Data are presented as mean ± SEM and was analyzed by one-way ANOVA with Tukey's post-hoc test or a two-tailed *t*-test, n = 4–6/group. * indicates $p < 0.05$, ** indicates $p < 0.01$, *** indicates $p < 0.001$ when making the indicated comparisons.

this study. The specificity of the antibody 504B3 for LPA has previously been demonstrated by using i) a competitive binding ELISA where the antibody was found to not have affinity for LPC, PA or various sphingosine species, ii) a cell based assay in which 504B3 blocked LPA-induced activation of LPA_1, LPA_2 and LPA_3 with an approximate ID_{50} of 30 nmol/L (Goldshmit et al., 2012), and iii) a kinetic exclusion assay in which 504B3 was found to bind various LPA species with apparent K_D values ranging from 0.88 nM to 14 nM with an apparent K_D of 3.1 nM for LPA 18:1 (Crack et al., 2014). 504B3 was recently found to bind 18:1 LPC and 18:1 PA with similar affinities to 18:1 LPA when using compensated interferometry (Ray et al., 2021). We have not assessed the levels of LPA, LPC or PA in the DRG in the current study, nor have we, or others, addressed the selectivity of 504B3 *in vivo*. Thus, the data generated with 504B3 should be interpreted with caution as there is a possibility that the effects of 504B3 are also partly due to interference with LPC or PA. If the antibody is binding 18:1 LPC *in vivo*, it is also possible that the anti-nociceptive effects of 504B3 are due to not only blocking LPA from binding its receptors, but also disruption of the LPC-autotaxin synthesis pathway of LPA. Interestingly, recent work assessing LPC in the synovial fluid of arthritis patients found that levels of 16:0 LPC were elevated and correlated to pain, but members of the 18-series of LPC were unchanged (Jacquot et al., 2021). This suggests that 18:0 LPC is not the dominant pronociceptive form of LPC in painful arthritis. This notion, and the effects of 504B3 together with the anti-nociceptive effects of the $LPA_{1/3}$ antagonist Ki-16425 and *Lpar1* deficiency, provide compelling support for a role of LPA in CAIA-induced hypersensitivity.

The close proximity of SGCs to DRG neuronal soma (approximately 20 nm) allows for unique SGC-neuron communication to modulate

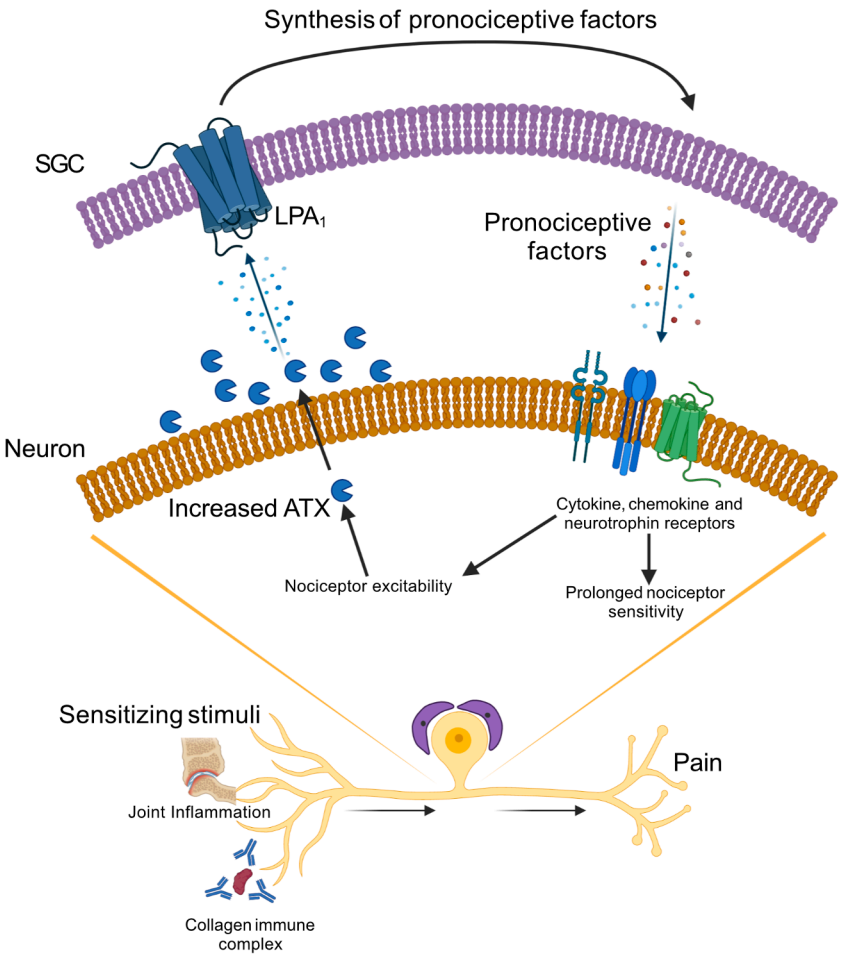

Fig. 10. Schematic of LPA signalling in CAIA. ATX is elevated in DRG neurons during the inflammatory and late neuropathic-like phases of CAIA, possibly in response to sensitizing stimuli like joint inflammation and immune complex activation of nociceptors. ATX in turn produces elevated levels of LPA that activates SGC-expressed LPA_1, leading to increased SGC activity. In response to LPA, SGCs produce increased levels of pronociceptive cytokines and NGF, which can then activate neuronally expressed cytokine and neurotrophin receptors. Activation of these receptors further promotes nociceptor excitability and prolong sensitization, leading the development of chronic pain.

sensory nerve signalling that is important for peripheral pain signalling and nociceptor sensitization (Takeda et al., 2009). Evidence of increased SGC activity, assessed by GFAP levels or SGC coupling via gap junctions, has been observed in inflammatory pain models (Blum et al., 2014; Nascimento et al., 2014), neuropathic pain models of nerve injury, chemotherapy, diabetes (Di Cesare Mannelli et al., 2013; Hanani et al., 2014; Warwick and Hanani, 2013), fibromyalgia (Goebel et al., 2021) and now rheumatoid arthritis. SGCs can modulate neuronal activity through regulating extracellular ion concentration and neuronal sensitization via cytokines (Takeda et al., 2009). Studies show that neurons can alter SGC activity through neuropeptide and ATP signalling (Chen et al., 2008; Hanani, 2005; Ji et al., 2013; Li et al., 2008; Takeda et al., 2009; Vause and Durham, 2010; Zhang et al., 2007), glutamate activation of SGC N-methyl-D-aspartate receptors (Castillo et al., 2013; Ferrari et al., 2014) and through fractalkine activation of SGC expressed CX3CR1 (Souza et al., 2013). Some of these stimuli, such as CGRP and fractalkine, increase SGC production of proinflammatory cytokines that sensitize neurons. Here we found increased neuronal ATX following CAIA induction, suggesting that neurons are responsible for elevated LPA. We then used pharmacological and genetic approaches to show LPA-LPA_1 signalling increases nociception-associated SGC activity *in vivo* and *in vitro* which could modulate neuronal activity to drive pain-like behavior during the inflammatory and late-phases of CAIA.

The role of LPA signalling during joint inflammation and destruction in other RA models has been previously investigated. For example, inhibition of ATX (Nikitopoulou et al., 2012) or LPA receptors (Miyabe et al., 2013; Nikitopoulou et al., 2013) reduces joint inflammation and destruction in the collagen-induced arthritis model. Here, we investigated a role for LPA in CAIA and RA-associated pain for the first time. In contrast to other models, we found that sequestering LPA/LPC/PA had no effect on CAIA-induced inflammation and $LPA_{1/3}$ antagonism only resolved inflammation slightly earlier than no treatment. CAIA also did not increase *Enpp2* expression in the ankle joint. Similarly, pharmacological blockade of ATX inhibits ankle bone erosion without reducing joint inflammation in TNF-transgenic mice (Flammier et al., 2019). While these results seem contradictory to what has been reported in the collagen-induced arthritis model, they could in fact be complimentary and explained by the different mechanisms underlying the two models. Collagen-induced arthritis is established by immunizing mice with type II collagen, which breaks the immune-tolerance, leading to activation of T-cells and B-cells and the production of anti-collagen type II antibodies. *In vitro* studies have found LPA is a chemoattractant factor for $CD4^+$ T-cells and can increase T-cell IL-13 (Georas, 2009; Lin and Boyce, 2006). Conversely, CAIA does not directly involve T-cell and B-cell activation, but instead mimics the effector phase of the disease when antibodies have already been generated (Krock et al., 2018). Thus, LPA may have two distinct roles in RA pathogenesis. In collagen-induced arthritis, LPA signalling appears to regulate the development and maintenance of inflammation and interference may prevent the generation of autoantibodies. In CAIA, our findings indicate that LPA signalling is not a major regulator of inflammation that is established and driven by anti-collagen antibodies.

Two remaining questions that warrant further studies are i) does LPC or PA contribute to pain pathophysiology in the CAIA model and ii) what is the trigger for sustained increased production of ATX and LPA? One hypothesis is that ATX generates LPA and acts in a very local environment, which in our case would suggest that neuronal ATX produces LPA in the DRG and then stimulates SGCs. This is in contrast to the proposed

mechanism of dorsal nerve root demyelination by ATX/LPA which includes LPA leaking from the spinal cord following partial sciatic nerve injury or intrathecal LPA (Inoue et al., 2004; Ueda, 2017). Recent single-cell RNA-seq studies have found that mouse DRG neurons express *Enpp2* (Thakur et al., 2014; Usoskin et al., 2014), which we confirmed with immunofluorescence. ATX expression is elevated during both the inflammatory and late phases of CAIA, thus there could be several drivers of ATX synthesis. Increased neuronal excitability and long-term transcriptional changes could contribute to elevated ATX in both phases while inflammatory pain mediators, such as cytokines and CGRP, may increase ATX during the inflammatory phase (Fig. 10). Future studies will investigate ATX regulation during the different phases of CAIA.

A limitation of our study is that only male mice were used. In fact, this is the case for the majority of studies aimed at investigating the role of LPA in pain mechanisms (Inoue et al., 2004; Ma et al., 2010b; McDougall et al., 2017; Ueda et al., 2018). Of note, LPA_1 is expressed by satellite glia cells in female humans, as we use a DRG from a female donor. Interestingly, in a recent study where the response to intra-articular injection of LPA to the knee joint was investigated in both sexes, it was found that female rats display increased signs of pain-like behavior and have greater nerve demyelination compared to male rats. Female rats also displayed a greater response to inhibition Na_v 1.8 currents following LPA injection (O'Brien et al., 2018). Thus, it is possible that inhibition of LPA signalling in female CAIA mice is more potent than in males. Sex differences between the role of the adaptive immune system versus spinal microglia in pain have been reported (Lopes et al., 2017; Rosen et al., 2017; Sorge et al., 2015) and we recently found that minocycline, a microglia inhibitor, attenuates mechanical hypersensitivity in male but not female CAIA mice (Fernandez-Zafra et al., 2018). However, potential sex-differences in SGC activity and regulation of pain have not yet been investigated. Future studies are warranted in order to determine if the role of LPA signalling and SGC in arthritis-associated pain-like behavior is subjected to sex dimorphism.

In conclusion we have found that satellite glial cells express LPA_1 in both human and mouse DRGs and that LPA alters SGC activity, which can modulate nociceptor activity. Interestingly, LPA signalling inhibition reduced signs of SGC activity, α2δ1 expression and pain-like behavior in the inflammatory and late phases of CAIA. Thus, the main conclusion from this study is that LPA signalling regulates CAIA-induced pain-like behavior by LPA activation of SGCs via LPA_1. A humanized antibody reported to be against LPA was well tolerated in a phase 1a clinical trial (NCT02341508) completed in 2016, but further development was not pursued. Regardless, this suggests that LPA signalling could be further developed as a therapeutic target for chronic pain. As persistent pain remains a problem for RA patients, new therapeutic strategies are needed. Interfering with LPA signalling or SGC activation could provide new strategies to manage RA-associated pain that is refractory to inflammation targeting therapies as well as pain in other autoimmune diseases.

Declaration of Competing Interest

RS is an inventor on compositions and uses of anti-LPA antibodies.

Acknowledgements

Funding: This work was supported by the Swedish Research Council (grant number 542-2013-8373) and the Knut and Alice Wallenberg Foundation (grant number 2012.0206 and 2018.0161), European Research Council (ERC) under the Horizon 2020 research and innovation programme (grant agreement number 866075), Ragnar Söderberg Foundation (grant number M138/12) and a donation from the Lundblad family (CIS); the Konung Gustaf V:s 80-year foundation, the International Association for the Study of Pain John J. Bonica Fellowship and a Canadian Institutes of Health Research fellowship (grant number MFE-171299) (EK); Swedish Brain Foundation (JS); Region Uppsala (ALF-grant and R&D funds), strategic funds Uppsala University and Magnus Bergvall Foundation (KK); and a United States Department of Defence (grant number W81XWH-17-1-0455 (to JC).

The authors would like to thank Katalin Sandor for assistance with experiments.

The 503B4 antibody was provided by Lpath, Inc.

Appendix A. Supplementary data

Supplementary data to this article can be found online at https://doi.org/10.1016/j.bbi.2022.01.003.

References

Ahmed, S., Magan, T., Vargas, M., Harrison, A., Sofat, N., 2014. Use of the painDETECT tool in rheumatoid arthritis suggests neuropathic and sensitization components in pain reporting. J. Pain Res. 7, 579–588. https://doi.org/10.2147/JPR.S69011.

Altawil, R., Saevarsdottir, S., Wedrén, S., Alfredsson, L., Klareskog, L., Lampa, J., 2016. Remaining Pain in Early Rheumatoid Arthritis Patients Treated With Methotrexate. Arthritis Care Res. (Hoboken) 68 (8), 1061–1068. https://doi.org/10.1002/acr.22790.

Bandoh, K., Aoki, J., Taira, A., Tsujimoto, M., Arai, H., Inoue, K., 2000. Lysophosphatidic acid (LPA) receptors of the EDG family are differentially activated by LPA species. FEBS Lett. 478, 159–165. https://doi.org/10.1016/S0014-5793(00)01827-5.

Bas, D.B., Su, J., Sandor, K., Agalave, N.M., Lundberg, J., Codeluppi, S., Baharpoor, A., Nandakumar, K.S., Holmdahl, R., Svensson, C.I., 2012. Collagen antibody–induced arthritis evokes persistent pain with spinal glial involvement and transient prostaglandin dependency. Arthritis Rheum. 64 (12), 3886–3896. https://doi.org/10.1002/art.37686.

Blum, E., Procacci, P., Conte, V., Hanani, M., 2014. Systemic inflammation alters satellite glial cell function and structure. A possible contribution to pain. Neuroscience 274, 209–217. https://doi.org/10.1016/J.NEUROSCIENCE.2014.05.029.

Boyle, D.L., Rosengren, S., Bugbee, W., Kavanaugh, A., Firestein, G.S., 2003. Quantitative biomarker analysis of synovial gene expression by real-time PCR. Arthritis Res Ther 5, 8. https://doi.org/10.1186/ar1004.

Castillo, C., Norcini, M., Martin Hernandez, L.A., Correa, G., Blanck, T.J.J., Recio-Pinto, E., 2013. Satellite glia cells in dorsal root ganglia express functional NMDA receptors. Neuroscience 240, 135–146. https://doi.org/10.1016/J.NEUROSCIENCE.2013.02.031.

Chaplan, S.R., Bach, F.W., Pogrel, J.W., Chung, J.M., Yaksh, T.L., 1994. Quantitative assessment of tactile allodynia in the rat paw. J Neurosci Methods 53 (1), 55–63.

Chen, Y., Zhang, X., Wang, C., Li, G., Gu, Y., Huang, L.-Y.-M., 2008. Activation of P2X7 receptors in glial satellite cells reduces pain through downregulation of P2X3 receptors in nociceptive neurons. Proc. Natl. Acad. Sci. U. S. A. 105 (43), 16773–16778. https://doi.org/10.1073/pnas.0801793105.

Choi, J.W., Herr, D.R., Noguchi, K., Yung, Y.C., Lee, C.-W., Mutoh, T., Lin, M.-E., Teo, S. T., Park, K.E., Mosley, A.N., Chun, J., 2010. LPA receptors: subtypes and biological actions. Annu. Rev. Pharmacol. Toxicol. 50 (1), 157–186. https://doi.org/10.1146/pharmtox.2010.50.issue-110.1146/annurev.pharmtox.010909.105753.

Contos, J.J.A., Fukushima, N., Weiner, J.A., Kaushal, D., Chun, J., 2000. Requirement for the lpA1 lysophosphatidic acid receptor gene in normal suckling behavior. Proc. Natl. Acad. Sci. U. S. A. 97 (24), 13384–13389. https://doi.org/10.1073/pnas.97.24.13384.

Cook, A.D., Rowley, M.J., Mackay, I.R., Gough, A., Emery, P., 1996. Antibodies to type II collagen in early rheumatoid arthritis. Correlation with disease progression. Arthritis Rheum. 39 (10), 1720–1727.

Crack, P.J., Zhang, M., Morganti-Kossmann, M., Morris, A.J., Wojciak, J.M., Fleming, J. K., Karve, I., Wright, D., Sashindranath, M., Goldshmit, Y., Conquest, A., Daglas, M., Johnston, L.A., Medcalf, R.L., Sabbadini, R.A., Pébay, A., 2014. Anti-lysophosphatidic acid antibodies improve traumatic brain injury outcomes. J. Neuroinflammation 11 (1), 37. https://doi.org/10.1186/1742-2094-11-37.

David, M., Machuca-Gayet, I., Kikuta, J., Ottewell, P., Mima, F., Leblanc, R., Bonnelye, E., Ribeiro, J., Holen, I., Vales, R.L., Jurdic, P., Chun, J., Clézardin, P., Ishii, M., Peyruchaud, O., 2014. Lysophosphatidic Acid Receptor Type 1 (LPA1) Plays a Functional Role in Osteoclast Differentiation and Bone Resorption Activity. J. Biol. Chem. 289 (10), 6551–6564. https://doi.org/10.1074/jbc.M113.533232.

Di Cesare Mannelli, L., Pacini, A., Bonaccini, L., Zanardelli, M., Mello, T., Ghelardini, C., 2013. Morphologic Features and Glial Activation in Rat Oxaliplatin-Dependent Neuropathic Pain. J. Pain 14 (12), 1585–1600. https://doi.org/10.1016/j.jpain.2013.08.002.

Dirig, D.M., Salami, A., Rathbun, M.L., Ozaki, G.T., Yaksh, T.L., 1997. Characterization of variables defining hindpaw withdrawal latency evoked by radiant thermal stimuli. J. Neurosci. Methods 76 (2), 183–191. https://doi.org/10.1016/S0165-0270(97)00097-6.

Edwards, R.R., Wasan, A.D., Bingham, C.O., Bathon, J., Haythornthwaite, J.A., Smith, M. T., Page, G.G., 2009. Enhanced reactivity to pain in patients with rheumatoid arthritis. Arthritis Res. Ther. 11 (3) https://doi.org/10.1186/ar2684.

Fernandez-Zafra, T., Gao, T., Jurczak, A., Sandor, K., Hore, Z., Agalave, N.M., Su, J., Estelius, J., Lampa, J., Hokfelt, T., Wiesenfeld-Hallin, Z., Xu, X., Denk, F., Svensson, C.I., 2018. Exploring the transcriptome of resident spinal microglia after collagen antibody-induced arthritis. Pain 160 (1), 224–236. https://doi.org/10.1097/j.pain.0000000000001394.

Ferrari, L.F., Lotufo, C.M., Araldi, D., Rodrigues, M.A., Macedo, L.P., Ferreira, S.H., Parada, C.A., 2014. Inflammatory sensitization of nociceptors depends on activation of NMDA receptors in DRG satellite cells. Proc. Natl. Acad. Sci. U. S. A. 111 (51), 18363–18368. https://doi.org/10.1073/pnas.1420601111.

Flammier, S., Peyruchaud, O., Bourguillault, F., Duboeuf, F., Davignon, J.-L., Norman, D. D., Isaac, S., Marotte, H., Tigyi, G., Machuca-Gayet, I., Coury, F., 2019. Osteoclast-Derived Autotaxin, a Distinguishing Factor for Inflammatory Bone Loss. Arthritis Rheumatol. (Hoboken, N.J.) 71, 1801–1811. https://doi.org/10.1002/art.41005.

Flatters, S.J.L., Bennett, G.J., 2004. Ethosuximide reverses paclitaxel- and vincristine-induced painful peripheral neuropathy. Pain 109, 150–161. https://doi.org/10.1016/j.pain.2004.01.029.

Fotopoulou, S., Oikonomou, N., Grigorieva, E., Nikitopoulou, I., Paparountas, T., Thanassopoulou, A., Zhao, Z., Xu, Y., Kontoyiannis, D.L., Remboutsika, E., Aidinis, V., 2010. ATX expression and LPA signalling are vital for the development of the nervous system. Dev. Biol. 339, 451–464. https://doi.org/10.1016/j.ydbio.2010.01.007.

Georas, S.N., 2009. Lysophosphatidic acid and autotaxin: emerging roles in innate and adaptive immunity. Immunol. Res. 45 (2-3), 229–238. https://doi.org/10.1007/s12026-009-8104-y.

Geraldo, L.H.M., Spohr, T.C.L.d.S., Amaral, R.F.d., Fonseca, A.C.C.d., Garcia, C., Mendes, F.d.A., Freitas, C., dosSantos, M.F., Lima, F.R.S., 2021. Role of lysophosphatidic acid and its receptors in health and disease: novel therapeutic strategies. Signal Transduct. Target. Ther. 6 (1) https://doi.org/10.1038/s41392-020-00367-5.

Goebel, A., Krock, E., Gentry, C., Cuhadar, U., Vastani, N., Sensi, S., Sandor, K., Jurczak, A., Baharpoor, A., Brieskorn, L., Urbina, C.M., Sandstrom, A., Tour, J., Kadetoff, D., Kosek, E., Bevan, S., Svensson, C.I., Andersson, D.A., 2021. Passive transfer of fibromyalgia symptoms from patients to mice. J. Clin. Invest. 131, e144201. Doi: 10.1172/JCI144201.

Goldshmit, Y., Matteo, R., Sztal, T., Ellett, F., Frisca, F., Moreno, K., Crombie, D., Lieschke, G.J., Currie, P.D., Sabbadini, R.A., Pébay, A., 2012. Blockage of Lysophosphatidic Acid Signaling Improves Spinal Cord Injury Outcomes. Am. J. Pathol. 181, 978–992. https://doi.org/10.1016/j.ajpath.2012.06.007.

Hanani, M., 2005. Satellite glial cells in sensory ganglia: from form to function. Brain Res. Brain Res. Rev. 48 (3), 457–476. https://doi.org/10.1016/j.brainresrev.2004.09.001.

Hanani, M., Blum, E., Liu, S., Peng, L., Liang, S., 2014. Satellite glial cells in dorsal root ganglia are activated in streptozotocin-treated rodents. J. Cell. Mol. Med. 18 (12), 2367–2371. https://doi.org/10.1111/jcmm.12406.

Harrison, S.M., Reavill, C., Brown, G., Brown, J.T., Cluderay, J.E., Crook, B., Davies, C. H., Dawson, L.A., Grau, E., Heidbreder, C., Hemmati, P., Hervieu, G., Howarth, A., Hughes, Z.A., Hunter, A.J., Latcham, J., Pickering, S., Pugh, P., Rogers, D.C., Shilliam, C.S., Maycox, P.R., 2003. LPA1 receptor-deficient mice have phenotypic changes observed in psychiatric disease. Mol. Cell. Neurosci. 24 (4), 1170–1179. https://doi.org/10.1016/j.mcn.2003.09.001.

Holmdahl, R., Malmström, V., Vuorio, E., 1993. Autoimmune recognition of cartilage collagens. Ann. Med. 25 (3), 251–264.

Inoue, M., Ma, L., Aoki, J., Chun, J., Ueda, H., 2008. Autotaxin, a synthetic enzyme of lysophosphatidic acid (LPA), mediates the induction of nerve-injured neuropathic pain. Mol. Pain 4, 6. https://doi.org/10.1186/1744-8069-4-6.

Inoue, M., Rashid, M.H., Fujita, R., Contos, J.J.A., Chun, J., Ueda, H., 2004. Initiation of neuropathic pain requires lysophosphatidic acid receptor signaling. Nat. Med. 10 (7), 712–718. https://doi.org/10.1038/nm1060.

Jacquot, F., Khoury, S., Labrum, B., Delanoe, K., Pidoux, L., Barbier, J., Delay, L., Bayle, A., Aissouni, Y., Barriere, D.A., Kultima, K., Freyhult, E., Hugo, A., Kosek, E., Ahmed, A.S., Jurczak, A., Lingueglia, E., Svensson, C.I., Breuil, V., Ferreira, T., Marchand, F., Deval, E., 2021. Lysophosphatidyl-choline 16:0 mediates persistent joint pain through Acid-Sensing Ion Channel 3: preclinical and clinical evidences. Pain 2021. In press.

Ji, R.-R., Berta, T., Nedergaard, M., 2013. Glia and pain: Is chronic pain a gliopathy? Pain 154, S10–S28. https://doi.org/10.1016/j.pain.2013.06.022.

Kano, K., Matsumoto, H., Inoue, A., Yukiura, H., Kanai, M., Chun, J., Ishii, S., Shimizu, T., Aoki, J., 2019. Molecular mechanism of lysophosphatidic acid-induced hypertensive response. Sci. Rep. 9, 2662. https://doi.org/10.1038/s41598-019-39041-4.

Kihara, Y., Maceyka, M., Spiegel, S., Chun, J., 2014. Lysophospholipid receptor nomenclature review: IUPHAR Review 8. Br. J. Pharmacol. 171 (15), 3575–3594. https://doi.org/10.1111/bph.12678.

Kim, W.U., Yoo, W.H., Park, W., Kang, Y.M., Kim, S.I., Park, J.H., Lee, S.S., Joo, Y.S., Min, J.K., Hong, Y.S., Lee, S.H., Park, S.H., Cho, C.S., Kim, H.Y., 2000. IgG antibodies to type II collagen reflect inflammatory activity in patients with rheumatoid arthritis. J. Rheumatol. 27, 575–581.

Koop, S.M.W., ten Klooster, P.M., Vonkeman, H.E., Steunebrink, L.M.M., van de Laar, M. A.F.J., 2015. Neuropathic-like pain features and cross-sectional associations in rheumatoid arthritis. Arthritis Res. Ther. 17, 237. https://doi.org/10.1186/s13075-015-0761-8.

Krock, E., Jurczak, A., Svensson, C.I., 2018. Pain pathogenesis in rheumatoid arthritis-what have we learned from animal models? Pain 159 (Suppl), S98–S109. https://doi.org/10.1097/j.pain.0000000000001333.

Le Maitre, E., Barde, S.S., Palkovits, M., Diaz-Heijtz, R., Hokfelt, T.G.M., 2013. Distinct features of neurotransmitter systems in the human brain with focus on the galanin system in locus coeruleus and dorsal raphe. Proc. Natl. Acad. Sci. 110 (6), E536–E545. https://doi.org/10.1073/pnas.1221378110.

Lee, Y.C., Cui, J., Lu, B., Frits, M.L., Iannaccone, C.K., Shadick, N.A., Weinblatt, M.E., Solomon, D.H., 2011. Pain persists in DAS28 rheumatoid arthritis remission but not in ACR/EULAR remission: a longitudinal observational study. Arthritis Res. Ther. 13 (3), R83. https://doi.org/10.1186/ar3353.

Li, J., Vause, C.V., Durham, P.L., 2008. Calcitonin gene-related peptide stimulation of nitric oxide synthesis and release from trigeminal ganglion glial cells. Brain Res. 1196, 22–32. https://doi.org/10.1016/j.brainres.2007.12.028.

Lin, D.A., Boyce, J.A., 2006. Lysophospholipids as Mediators of Immunity, in: Alt, F.W., Austen, K.F., Honjo, T., Melchers, F., Uhr, J.W., Unanue, E.R.B.T.-A. in I. (Eds.), . Academic Press, pp. 141–167. Doi: 10.1016/S0065-2776(05)89004-2.

Lin, M.-E., Rivera, R.R., Chun, J., 2012. Targeted deletion of LPA5 identifies novel roles for lysophosphatidic acid signaling in development of neuropathic pain. J. Biol. Chem. 287 (21), 17608–17617. https://doi.org/10.1074/jbc.M111.330183.

Lindh, I., Snir, O., Lönnblom, E., Uysal, H., Andersson, I., Nandakumar, K., Vierboom, M., 't Hart, B., Malmström, V., Holmdahl, R., 2014. Type II collagen antibody response is enriched in the synovial fluid of rheumatoid joints and directed to the same major epitopes as in collagen induced arthritis in primates and mice. Arthritis Res. Ther. 16 (4), R143. https://doi.org/10.1186/ar4605.

Livak, K.J., Schmittgen, T.D., 2001. Analysis of Relative Gene Expression Data Using Real-Time Quantitative PCR and the 2−ΔΔCT Method. Methods 25, 402–408. https://doi.org/10.1006/meth.2001.1262.

Lopes, D.M., Malek, N., Edye, M., Jager, S.B., McMurray, S., McMahon, S.B., Denk, F., 2017. Sex differences in peripheral not central immune responses to pain-inducing injury. Sci. Rep. 7, 16460. https://doi.org/10.1038/s41598-017-16664-z.

Ma, L., Nagai, J., Ueda, H., 2010a. Microglial activation mediates de novo lysophosphatidic acid production in a model of neuropathic pain. J. Neurochem. 115, 643–653. https://doi.org/10.1111/j.1471-4159.2010.06955.x.

Ma, L., Uchida, H., Nagai, J., Inoue, M., Aoki, J., Ueda, H., 2010b. Evidence for de novo synthesis of lysophosphatidic acid in the spinal cord through phospholipase A2 and autotaxin in nerve injury-induced neuropathic pain. J. Pharmacol. Exp. Ther. 333 (2), 540–546. https://doi.org/10.1124/jpet.109.164830.

Malin, S.A., Davis, B.M., Molliver, D.C., 2007. Production of dissociated sensory neuron cultures and considerations for their use in studying neuronal function and plasticity. Nat. Protoc. 2 (1), 152–160. https://doi.org/10.1038/nprot.2006.461.

McDougall, J.J., Albacete, S., Schuelert, N., Mitchell, P.G., Lin, C., Oskins, J.L., Bui, H.H., Chambers, M.G., 2017. Lysophosphatidic acid provides a missing link between osteoarthritis and joint neuropathic pain. Osteoarthr. Cartil. 25 (6), 926–934. https://doi.org/10.1016/j.joca.2016.08.016.

Miyabe, Y., Miyabe, C., Iwai, Y., Takayasu, A., Fukuda, S., Yokoyama, W., Nagai, J., Jona, M., Tokuhara, Y., Ohkawa, R., Albers, H.M., Ovaa, H., Aoki, J., Chun, J., Yatomi, Y., Ueda, H., Miyasaka, M., Miyasaka, N., Nanki, T., 2013. Necessity of lysophosphatidic acid receptor 1 for development of arthritis. Arthritis Rheum. 65 (8), 2037–2047. https://doi.org/10.1002/art.37991.

Mizuno, H., Kihara, Y., Kussrow, A., Chen, A., Ray, M., Rivera, R., Bornhop, D.J., Chun, J., 2019. Lysophospholipid G protein-coupled receptor binding parameters as determined by backscattering interferometry. J. Lipid Res. 60 (1), 212–217. https://doi.org/10.1194/jlr.D089938.

Mullazehi, M., Wick, M.C., Klareskog, L., van Vollenhoven, R., Rönnelid, J., 2012. Anti-type II collagen antibodies are associated with early radiographic destruction in rheumatoid arthritis. Arthritis Res. Ther. 14 (3), R100. https://doi.org/10.1186/ar3825.

Nagai, J., Uchida, H., Matsushita, Y., Yano, R., Ueda, M., Niwa, M., Aoki, J., Chun, J., Ueda, H., 2010. Autotaxin and lysophosphatidic acid1 receptor-mediated demyelination of dorsal root fibers by sciatic nerve injury and intrathecal lysophosphatidylcholine. Mol. Pain 6, 78. https://doi.org/10.1186/1744-8069-6-78.

Nandakumar, K.S., Holmdahl, R., 2007. Collagen antibody induced arthritis. Methods Mol. Med. 136, 215–223.

Nascimento, D.S.M., Castro-Lopes, J.M., Neto, F.L.M., Arai, K., 2014. Satellite Glial Cells Surrounding Primary Afferent Neurons Are Activated and Proliferate during Monoarthritis in Rats: Is There a Role for ATF3? PLoS One 9 (9), e108152.

Nguyen, M.Q., von Buchholtz, L.J., Reker, A.N., Ryba, N.J.P., Davidson, S., 2021. Single-nucleus transcriptomic analysis of human dorsal root ganglion neurons. Elife 10, e71752. Doi: 10.7554/eLife.71752.

Nikitopoulou, I., Kaffe, E., Sevastou, I., Sirioti, I., Samiotaki, M., Madan, D., Prestwich, G. D., Aidinis, V., 2013. A metabolically-stabilized phosphonate analog of lysophosphatidic acid attenuates collagen-induced arthritis. PLoS One 8, e70941. https://doi.org/10.1371/journal.pone.0070941.

Nikitopoulou, I., Oikonomou, N., Karouzakis, E., Sevastou, I., Nikolaidou-Katsaridou, N., Zhao, Z., Mersinias, V., Armaka, M., Xu, Y., Masu, M., Mills, G.B., Gay, S., Kollias, G., Aidinis, V., 2012. Autotaxin expression from synovial fibroblasts is essential for the pathogenesis of modeled arthritis. J. Exp. Med. 209, 925–933. https://doi.org/10.1084/jem.20112012.

Noguchi, K., Herr, D., Mutoh, T., Chun, J., 2009. Lysophosphatidic acid (LPA) and its receptors. Curr. Opin. Pharmacol. 9 (1), 15–23. https://doi.org/10.1016/j.coph.2008.11.010.

O'Brien, M.S., Philpott, H.T.A., McDougall, J.J., 2018. Targeting The NaV1.8 ion Channel Engenders Sex-Specific Responses in Lysophosphatidic Acid-Induced Joint Neuropathy. Pain. 160 (1), 269–278. https://doi.org/10.1097/j.pain.0000000000001399.

Ohara, P.T., Vit, J.-P., Bhargava, A., Romero, M., Sundberg, C., Charles, A.C., Jasmin, L., 2009. Gliopathic pain: when satellite glial cells go bad. Neuroscientist 15 (5), 450–463. https://doi.org/10.1177/1073858409336094.

Orosa, B., García, S., Martínez, P., González, A., Gómez-Reino, J.J., Conde, C., 2014. Lysophosphatidic acid receptor inhibition as a new multipronged treatment for rheumatoid arthritis. Ann. Rheum. Dis. 73 (1), 298–305. https://doi.org/10.1136/annrheumdis-2012-202832.

Orosa, B., González, A., Mera, A., Gómez-Reino, J.J., Conde, C., 2012. Lysophosphatidic acid receptor 1 suppression sensitizes rheumatoid fibroblast-like synoviocytes to

tumor necrosis factor-induced apoptosis. Arthritis Rheum. 64 (8), 2460–2470. https://doi.org/10.1002/art.34443.
Palmer, C.R., Liu, C.S., Romanow, W.J., Lee, M.-H., Chun, J., 2021. Altered cell and RNA isoform diversity in aging Down syndrome brains. Proc. Natl. Acad. Sci. U. S. A. 118. Doi: 10.1073/pnas.2114326118.
Pollard, L.C., Ibrahim, F., Choy, E.H., Scott, D.L., 2012. Pain thresholds in rheumatoid arthritis: the effect of tender point counts and disease duration. J. Rheumatol. 39 (1), 28–31. https://doi.org/10.3899/jrheum.110668.
Ray, M., Kihara, Y., Bornhop, D.J., Chun, J., 2021. Lysophosphatidic acid (LPA)-antibody (504B3) engagement detected by interferometry identifies off-target binding. Lipids Health Dis. 20, 32. https://doi.org/10.1186/s12944-021-01454-4.
Ray, M., Nagai, K., Kihara, Y., Kussrow, A., Kammer, M.N., Frantz, A., Bornhop, D.J., Chun, J., 2020. Unlabeled lysophosphatidic acid receptor binding in free solution as determined by a compensated interferometric reader. J. Lipid Res. 61 (8), 1244–1251. https://doi.org/10.1194/jlr.D120000880.
Rivera, R.R., Lin, M.-E., Bornhop, E.C., Chun, J., 2020. Conditional Lpar1 gene targeting identifies cell types mediating neuropathic pain. FASEB J. 34 (7), 8833–8842. https://doi.org/10.1096/fsb2.v34.710.1096/fj.202000317R.
Robering, J.W., Gebhardt, L., Wolf, K., Kühn, H., Kremer, A.E., Fischer, M.J.M., 2019. Lysophosphatidic acid activates satellite glia cells and Schwann cells. Glia 67 (5), 999–1012. https://doi.org/10.1002/glia.v67.510.1002/glia.23585.
Rosen, S., Ham, B., Mogil, J.S., 2017. Sex differences in neuroimmunity and pain. J. Neurosci. Res. 95, 500–508. https://doi.org/10.1002/jnr.23831.
Sánchez-Marín, L., Ladrón de Guevara-Miranda, D., Mañas-Padilla, M.C., Alén, F., Moreno-Fernández, R.D., Díaz-Navarro, C., Pérez-del Palacio, J., García-Fernández, M., Pedraza, C., Pavón, F.J., Rodríguez de Fonseca, F., Santín, L.J., Serrano, A., Castilla-Ortega, E., 2018. Systemic blockade of LPA1/3 lysophosphatidic acid receptors by ki16425 modulates the effects of ethanol on the brain and behavior. Neuropharmacology 133, 189–201. https://doi.org/10.1016/J.NEUROPHARM.2018.01.033.
Savaskan, N.E., Rocha, L., Kotter, M.R., Baer, A., Lubec, G., van Meeteren, L.A., Kishi, Y., Aoki, J., Moolenaar, W.H., Nitsch, R., Bräuer, A.U., 2007. Autotaxin (NPP-2) in the brain: cell type-specific expression and regulation during development and after neurotrauma. Cell. Mol. Life Sci. 64 (2), 230–243. https://doi.org/10.1007/s00018-006-6412-0.
Sim, M.K., Kim, D.-Y., Yoon, J., Park, D.H., Kim, Y.-G., 2014. Assessment of peripheral neuropathy in patients with rheumatoid arthritis who complain of neurologic symptoms. Ann. Rehabil. Med. 38, 249–255. https://doi.org/10.5535/arm.2014.38.2.249.
Sorge, R.E., Mapplebeck, J.C.S., Rosen, S., Beggs, S., Taves, S., Alexander, J.K., Martin, L. J., Austin, J.-S., Sotocinal, S.G., Chen, D.i., Yang, M.u., Shi, X.Q., Huang, H., Pillon, N.J., Bilan, P.J., Tu, Y., Klip, A., Ji, R.-R., Zhang, J.i., Salter, M.W., Mogil, J.S., 2015. Different immune cells mediate mechanical pain hypersensitivity in male and female mice. Nat. Neurosci. 18 (8), 1081–1083. https://doi.org/10.1038/nn.4053.
Souza, G.R., Talbot, J., Lotufo, C.M., Cunha, F.Q., Cunha, T.M., Ferreira, S.H., 2013. Fractalkine mediates inflammatory pain through activation of satellite glial cells. Proc. Natl. Acad. Sci. U. S. A. 110 (27), 11193–11198. https://doi.org/10.1073/pnas.1307445110.
Srikanth, M., Chew, W.S., Hind, T., Lim, S.M., Hay, N.W.J., Lee, J.H.M., Rivera, R., Chun, J., Ong, W.-Y., Herr, D.R., 2018. Lysophosphatidic acid and its receptor LPA (1) mediate carrageenan induced inflammatory pain in mice. Eur. J. Pharmacol. 841, 49–56. https://doi.org/10.1016/j.ejphar.2018.10.005.
Su, J., Gao, T., Shi, T., Xiang, Q., Xu, X., Wiesenfeld-Hallin, Z., Hökfelt, T., Svensson, C.I., 2015. Phenotypic changes in dorsal root ganglion and spinal cord in the collagen antibody-induced arthritis mouse model. J. Comp. Neurol. 523 (10), 1505–1528. https://doi.org/10.1002/cne.23749.
Su, J., Sandor, K., Skold, K., Hokfelt, T., Svensson, C.I., Kultima, K., 2014. Identification and quantification of neuropeptides in naive mouse spinal cord using mass spectrometry reveals [des-Ser1]-cerebellin as a novel modulator of nociception. J. Neurochem. 130, 199–214. https://doi.org/10.1111/jnc.12730.
Svensson, C.I., Fitzsimmons, B., Azizi, S., Powell, H.C., Hua, X.Y., Yaksh, T.L., 2005. Spinal p38β isoform mediates tissue injury-induced hyperalgesia and spinal sensitization. J. Neurochem. 92, 1508–1520. https://doi.org/10.1111/j.1471-4159.2004.02996.x.
Takeda, M., Takahashi, M., Matsumoto, S., 2009. Contribution of the activation of satellite glia in sensory ganglia to pathological pain. Neurosci. Biobehav. Rev. 33 (6), 784–792. https://doi.org/10.1016/j.neubiorev.2008.12.005.
Taylor, P., Manger, B., Alvaro-Gracia, J., Johnstone, R., Gomez-Reino, J., Eberhardt, E., Wolfe, F., Schwartzman, S., Furfaro, N., Kavanaugh, A., 2010. Patient perceptions concerning pain management in the treatment of rheumatoid arthritis. J. Int. Med. Res. 38 (4), 1213–1224. https://doi.org/10.1177/147323001003800402.
Thakur, M., Crow, M., Richards, N., Davey, G.I.J., Levine, E., Kelleher, J.H., Agley, C.C., Denk, F., Harridge, S.D.R., McMahon, S.B., 2014. Defining the nociceptor transcriptome. Front. Mol. Neurosci.
Tokumura, A., Majima, E., Kariya, Y., Tominaga, K., Kogure, K., Yasuda, K., Fukuzawa, K., 2002. Identification of human plasma lysophospholipase D, a lysophosphatidic acid-producing enzyme, as autotaxin, a multifunctional phosphodiesterase. J. Biol. Chem. 277 (42), 39436–39442. https://doi.org/10.1074/jbc.M205623200.
Ueda, H., 2017. Lysophosphatidic acid signaling is the definitive mechanism underlying neuropathic pain. Pain 158 (Suppl), S55–S65. https://doi.org/10.1097/j.pain.0000000000000813.
Ueda, H., Neyama, H., Nagai, J., Matsushita, Y., Tsukahara, T., Tsukahara, R., 2018. Involvement of lysophosphatidic acid-induced astrocyte activation underlying the maintenance of partial sciatic nerve injury-induced neuropathic pain. Pain 159 (11), 2170–2178. https://doi.org/10.1097/j.pain.0000000000001316.
Umezu-Goto, M., Kishi, Y., Taira, A., Hama, K., Dohmae, N., Takio, K., Yamori, T., Mills, G.B., Inoue, K., Aoki, J., Arai, H., 2002. Autotaxin has lysophospholipase D activity leading to tumor cell growth and motility by lysophosphatidic acid production. J. Cell Biol. 158, 227 LP – 233.
Usoskin, D., Furlan, A., Islam, S., Abdo, H., Lönnerberg, P., Lou, D., Hjerling-Leffler, J., Haeggström, J., Kharchenko, O., Kharchenko, P.V., Linnarsson, S., Ernfors, P., 2014. Unbiased classification of sensory neuron types by large-scale single-cell RNA sequencing. Nat. Neurosci. 18 (1), 145–153.
Vause, C.V., Durham, P.L., 2010. Calcitonin gene-related peptide differentially regulates gene and protein expression in trigeminal glia cells: findings from array analysis. Neurosci. Lett. 473 (3), 163–167. https://doi.org/10.1016/j.neulet.2010.01.074.
Vierboom, M.P.M., Jonker, M., Bontrop, R.E., 't Hart, B., 2005. Modeling human arthritic diseases in nonhuman primates. Arthritis Res. Ther. 7, 145. https://doi.org/10.1186/ar1773.
Warwick, R.A., Hanani, M., 2013. The contribution of satellite glial cells to chemotherapy-induced neuropathic pain. Eur. J. Pain 17 (4), 571–580. https://doi.org/10.1002/ejp.2013.17.issue-410.1002/j.1532-2149.2012.00219.x.
Weiner, J.A., Chun, J., 1999. Schwann cell survival mediated by the signaling phospholipid lysophosphatidic acid. Proc. Natl. Acad. Sci. 96, 5233 LP – 5238. https://doi.org/10.1073/pnas.96.9.5233.
Weiner, J.A., Fukushima, N., Contos, J.J.A., Scherer, S.S., Chun, J., 2001. Regulation of Schwann Cell Morphology and Adhesion by Receptor-Mediated Lysophosphatidic Acid Signaling. J. Neurosci. 21, 7069 LP – 7078. Doi: 10.1523/JNEUROSCI.21-18-07069.2001.
Weiner, J.A., Hecht, J.H., Chun, J., 1998. Lysophosphatidic acid receptor gene vzg-1/lpA1/edg-2 is expressed by mature oligodendrocytes during myelination in the postnatal murine brain. J. Comp. Neurol. 398, 587–598. https://doi.org/10.1002/(SICI)1096-9861(19980907)398:4<587::AID-CNE10>3.0.CO;2-5.
Yung, Y.C., Stoddard, N.C., Chun, J., 2014. LPA receptor signaling: pharmacology, physiology, and pathophysiology. J. Lipid Res. 55 (7), 1192–1214. https://doi.org/10.1194/jlr.R046458.
Zeisel, A., Hochgerner, H., Lönnerberg, P., Johnsson, A., Memic, F., van der Zwan, J., Häring, M., Braun, E., Borm, L.E., La Manno, G., Codeluppi, S., Furlan, A., Lee, K., Skene, N., Harris, K.D., Hjerling-Leffler, J., Arenas, E., Ernfors, P., Marklund, U., Linnarsson, S., 2018. Molecular Architecture of the Mouse Nervous System. Cell 174 (4), 999–1014.e22. https://doi.org/10.1016/j.cell.2018.06.021.
Zhang, X., Chen, Y., Wang, C., Huang, L.-Y.- M., 2007. Neuronal somatic ATP release triggers neuron-satellite glial cell communication in dorsal root ganglia. Proc. Natl. Acad. Sci. U. S. A. 104 (23), 9864–9869. https://doi.org/10.1073/pnas.0611048104.